SAINT Technology Development in the Scope of LUVOIR

Brian A. Hicks

University of Maryland College Park
NASA Goddard Space Flight Center

February 15, 2017

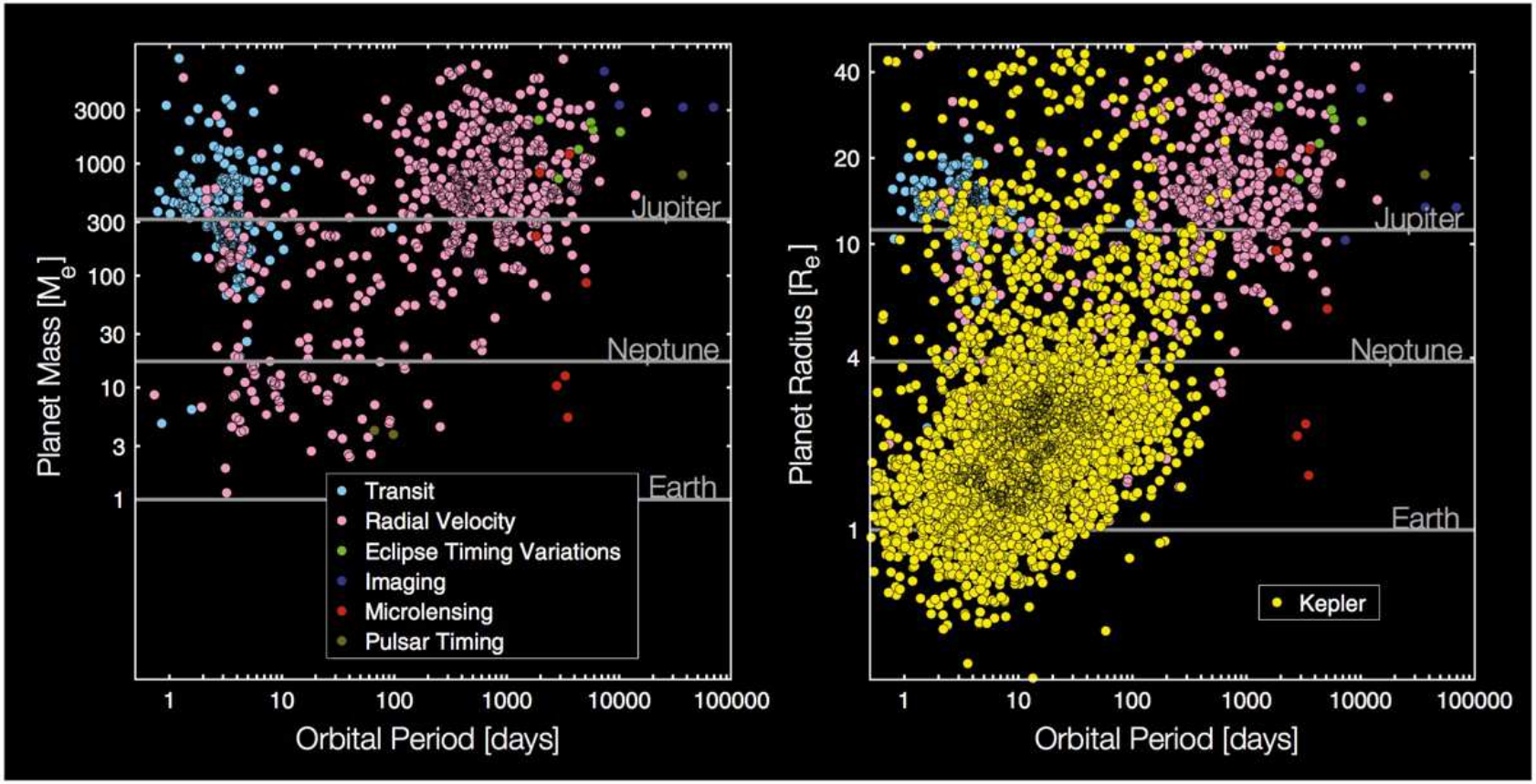

Fig. 1. Non-Kepler exoplanet discoveries (*Left*) are plotted as mass versus orbital period, colored according to the detection technique. A simplified mass–radius relation is used to transform planetary mass to radius (*Right*), and the >3,500 *Kepler* discoveries (yellow) are added for comparison. Eighty-six percent of the non-*Kepler* discoveries are larger than Neptune, whereas the inverse is true of the *Kepler* discoveries: 85% are smaller than Neptune.

Batahla *PNAS* **111** 12647–12654 (2014)

A sampling of imaged planetary systems

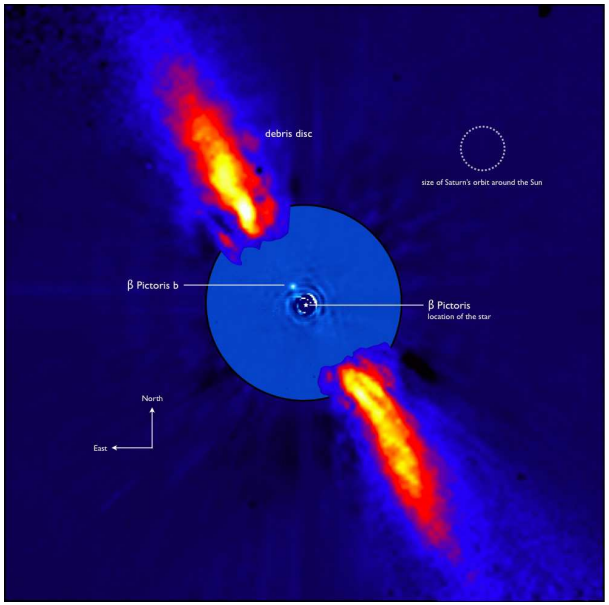

www.eso.org/public/images/eso0842b/

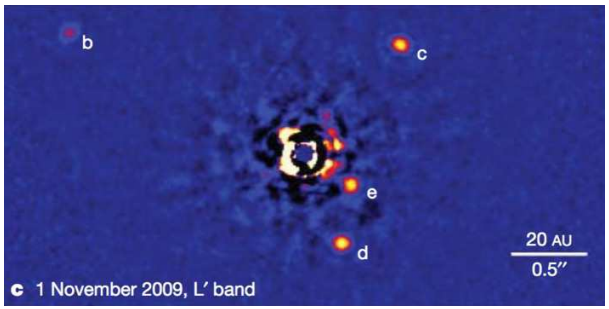

Marois+ *Nature* **468** (2010)

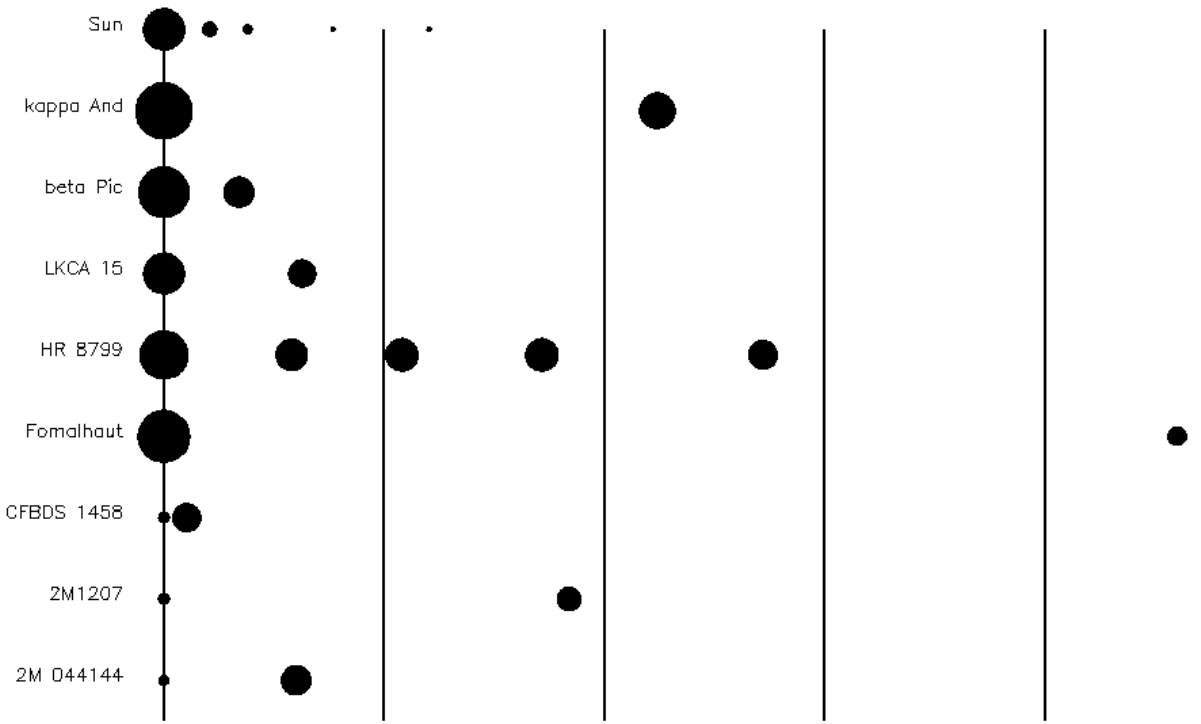

- Stellar sizes and planet sizes are shown on a different scale - orbital distances are shown scaled to the Solar System gas giants
- Typically younger (self-luminous) planets that are more massive and orbiting at large separations with century-scale periods

Contrast and resolution requirements

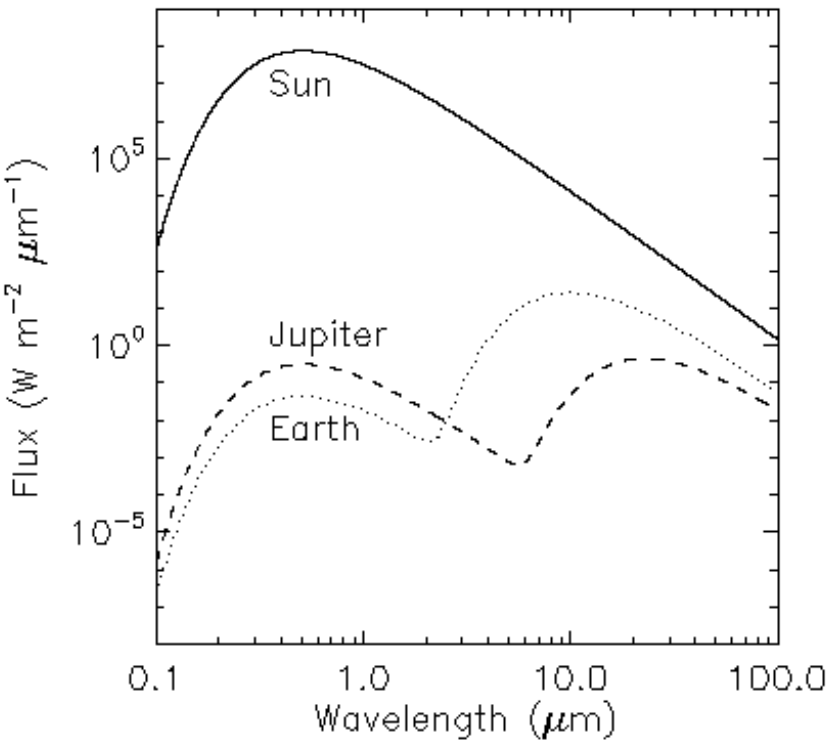

On-sky contrast determined from the sum of reflected light and thermal emission:

$$C(\Delta\lambda, t) = \int_{\Delta\lambda} \frac{\phi(t) A(\lambda) R_p^2}{d(t)^2} + \frac{R_p^2 B_p(\lambda, T_p)}{R_s^2 B_s(\lambda, T_s)} d\lambda$$

Determine aperture based on assumptions:

- λ_{max} = 750 nm
- Inner Working Angle (IWA) = $2\lambda/D$
- distance limit: 30 pc (97.9 ly)
- mean HZ separation for a Sun-like (G-type) star: 1.0 AU

$\rightarrow \theta_{max}$ =(1.0 AU)/(30 pc)=33 mas

$\rightarrow D_{min} = \frac{2(7.5\times10^{-7}\text{m})}{(0.033'')/(206265''\ \text{rad}^{-1})} = 9.4$ m

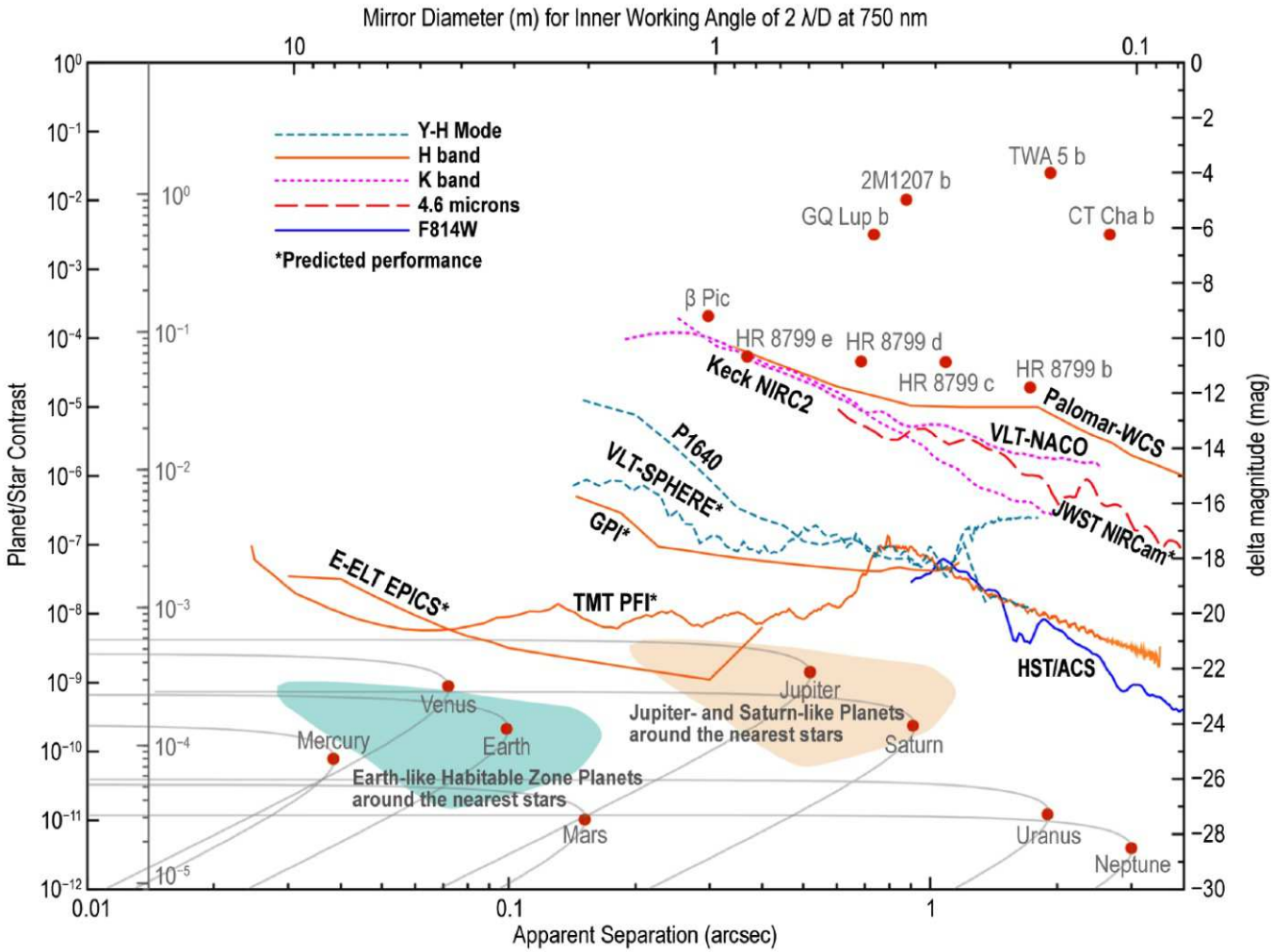

Lawson+ *Exoplanet Exploration Technology Plan* (2013)

High Contrast Imaging with the JWST NIRCAM Coronagraph

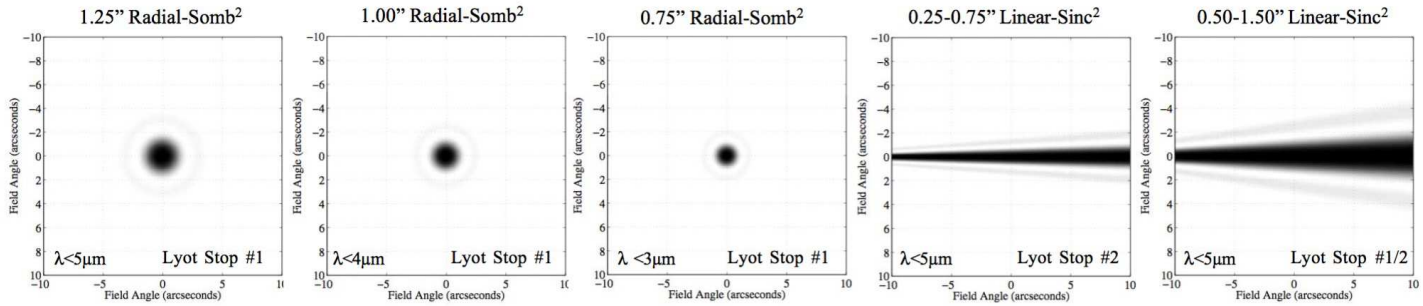

Figure 4. The NIRCAM occulting spot designs are shown along with the optical-filter compatibility range and Lyot stop requirement. The Lyot stop designs are shown in Fig. 5.

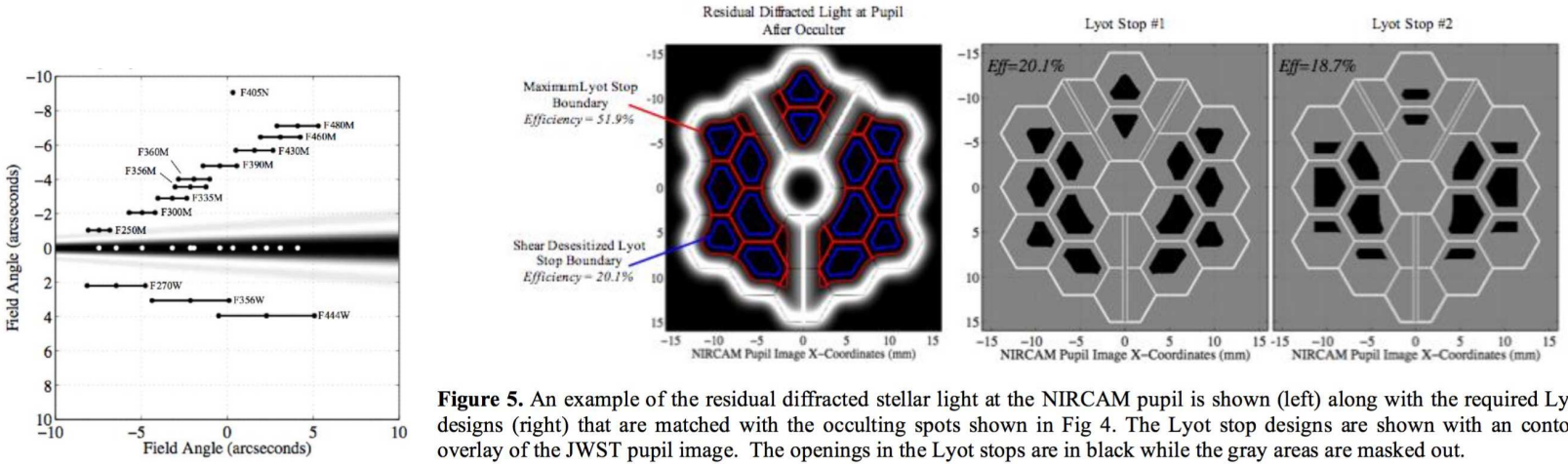

Figure 5. An example of the residual diffracted stellar light at the NIRCAM pupil is shown (left) along with the required Lyot stop designs (right) that are matched with the occulting spots shown in Fig 4. The Lyot stop designs are shown with an contour line overlay of the JWST pupil image. The openings in the Lyot stops are in black while the gray areas are masked out.

Green+ *Proc. SPIE* **5905** (2005)

The first space-based coronagraph equipped with a deformable mirror

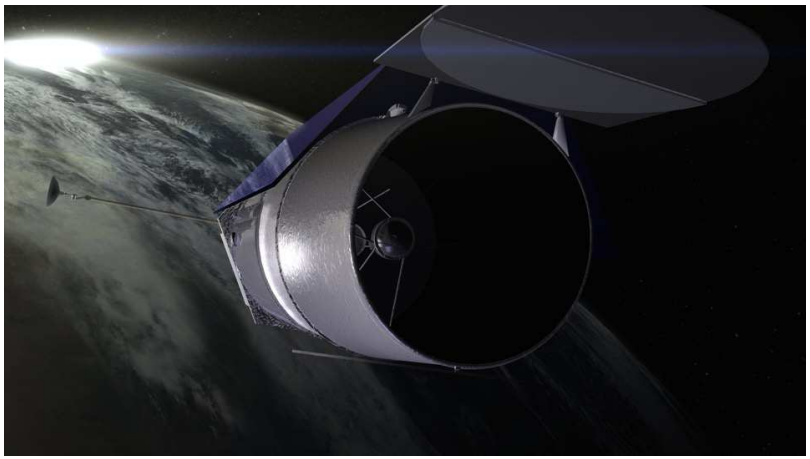

- 2.4 m aperture telescope
- Two coronagraphs alternately operated within a single optical beam-train:
  1. Hybrid Lyot Coronagraph (HLC) – planet imaging
  2. Shaped Pupil Coronagraph (SPC) – planet spectroscopy & disk characterization

Bandpass	430–980 nm	Measured sequentially in 10% and 18% bands
Inner Working Angle [radial]	150 mas 270 mas	at 550 nm, 3/D driven by AFTA pupil obscurations at 1 μm (imaging camera)
Outer Working Angle [radial]	0.5 arcsec 0.9 arcsec	at 550 nm, $10\lambda/D$, driven by 48 × 48 format DM at 1 μm (imaging camera)
Detection Limit (Contrast)	10^{-9}	Cold Jupiters; deeper contrast unlikely due to pupil shape & extreme stability requirements
Spectral Resolution	70	$R = \lambda/\delta\lambda$ (IFS)
IFS Spatial Sampling	17 mas	3 lenslets per λ/D, better than Nyquist

Hybrid Lyot Coronagraph (HLC)

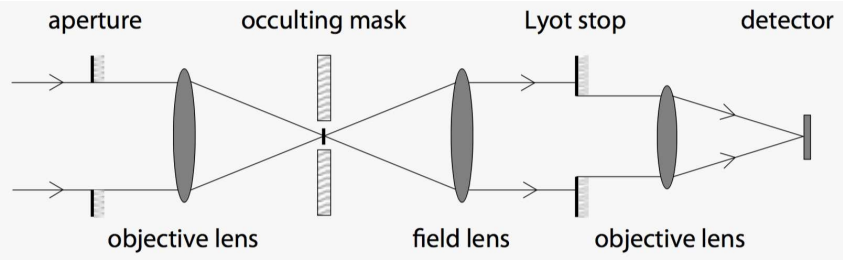

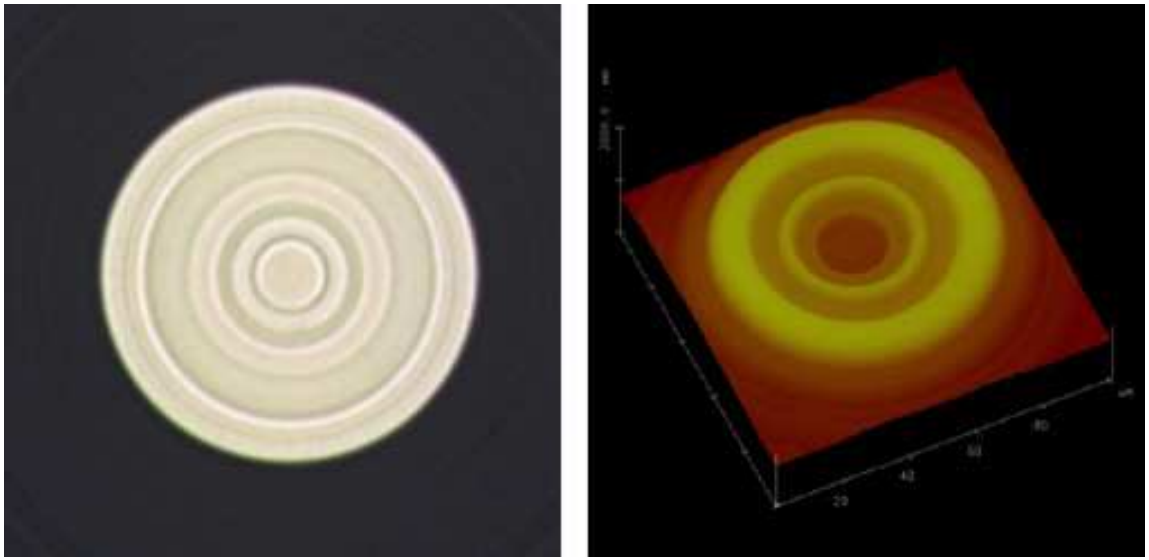

Microscope photo and atomic force microscope surface profile of an e-beam fabricated occulting mask for the WFIRST-coronagraph from:
microdevices.jpl.nasa.govcapabilitiesoptical-componentscoronagraph-occulting-masks.php

Shaped Pupil Coronagraph (SPC)

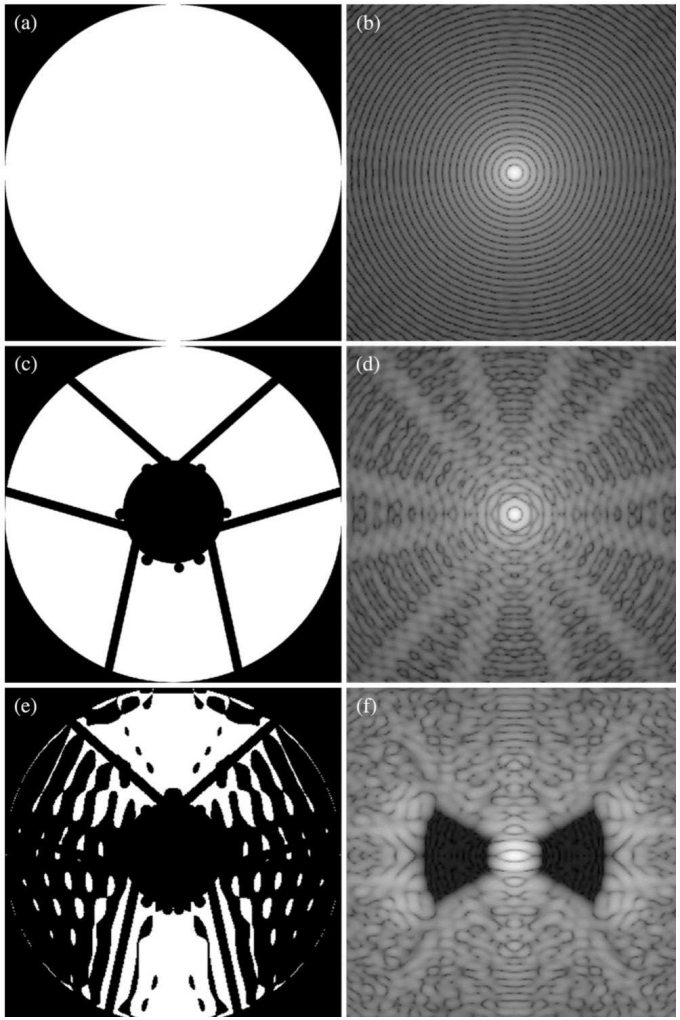

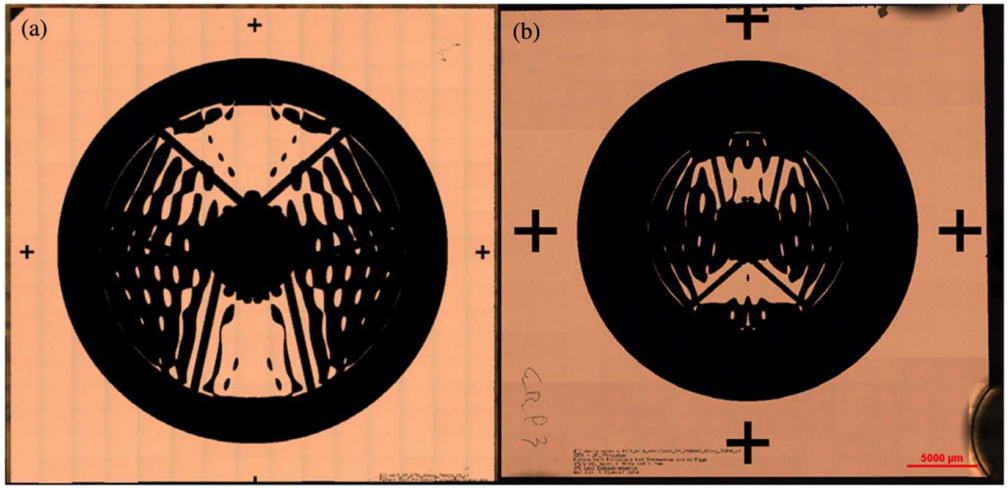

Figures from Cady+ *JATIS* **2** 011004 (2016)

Large UV-Optical-IR (LUVOIR) Telescope

- A general astrophysics surveyor that is likely to leverage the substantial investment in deployable hexagonal segment space telescope architecture developed for JWST
- Challenging stability ($\sim$ 10 pm) requirements over long observation periods (days to weeks) needed to characterize exoplanet atmospheres

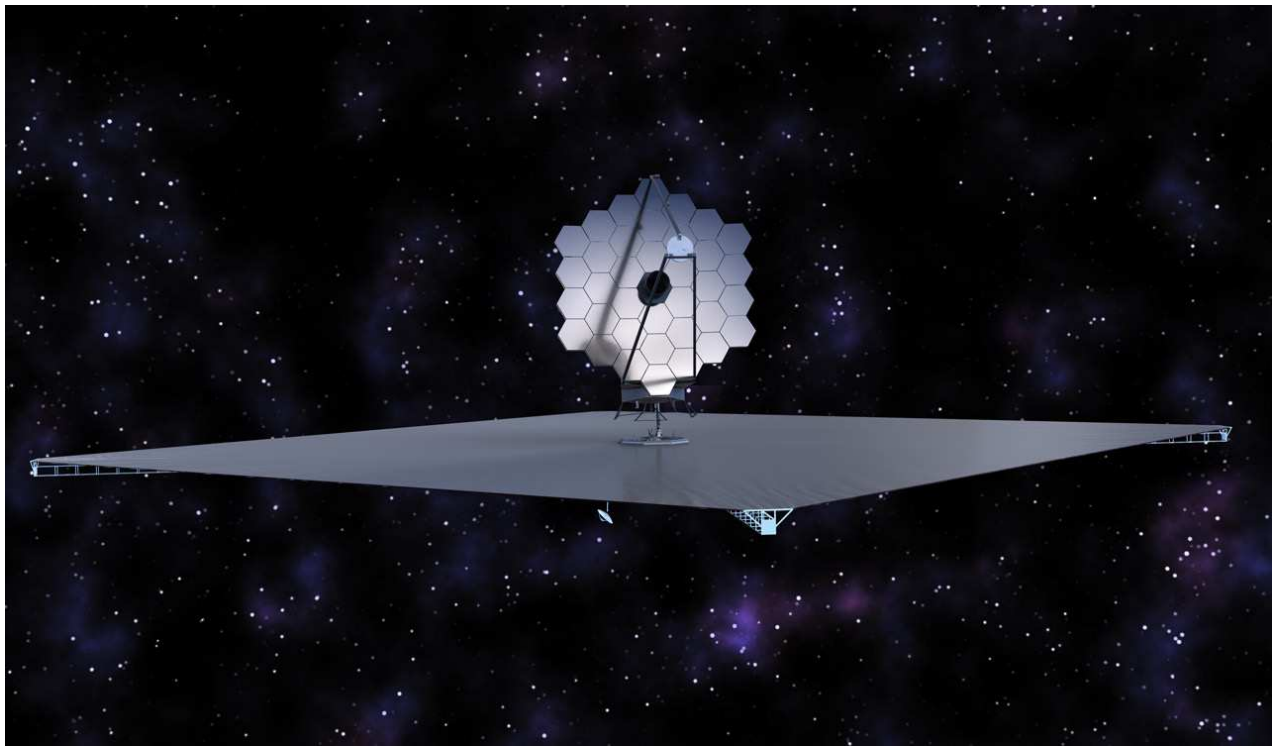

Approaches to high-contrast with segmented apertures

APLC/SP
Diffraction

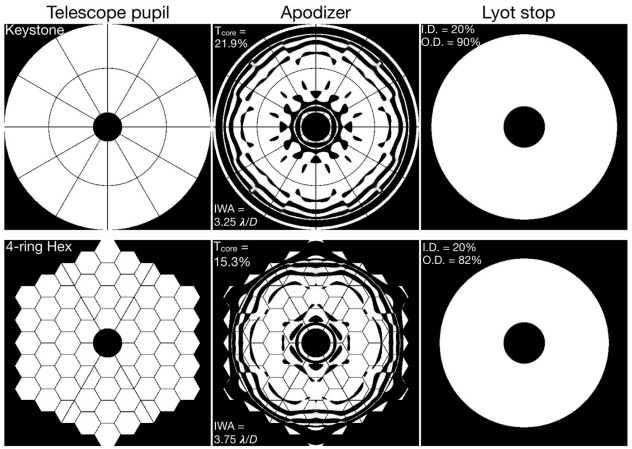

Courtesy of Neil Zimmerman
Submitted to SCDA Study Report

PIAA
Beam densification (remapping)

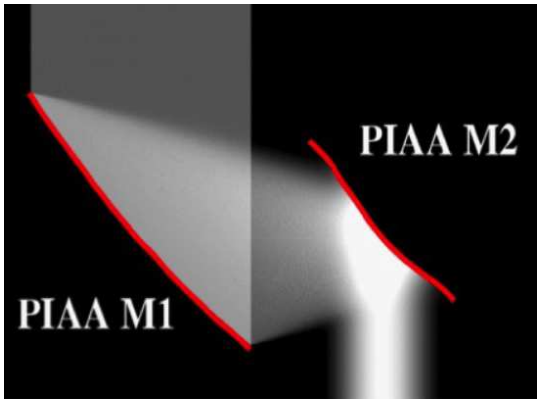

Guyon+ **ApJ** (2005)

VNC
Destructive interference

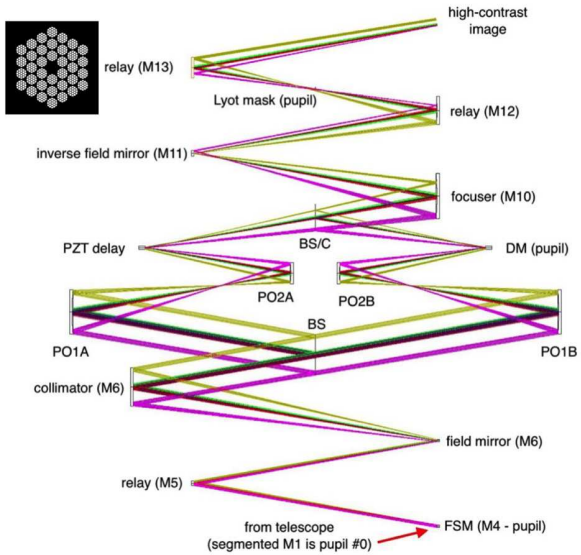

Hicks+ **Proc SPIE** (2016)

Starlight suppression with a nulling interferometer

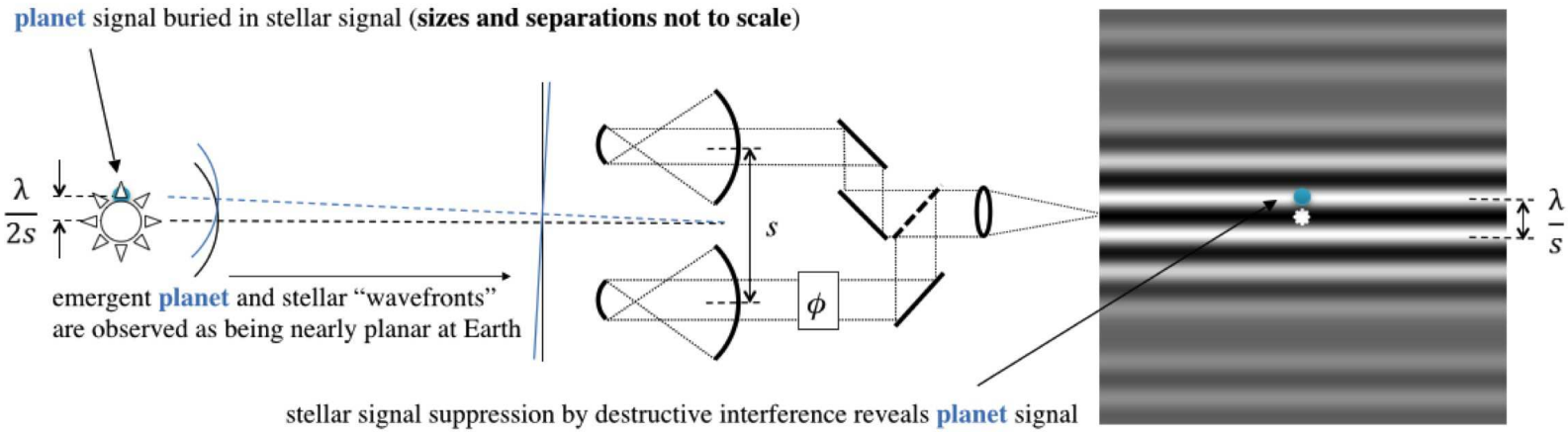

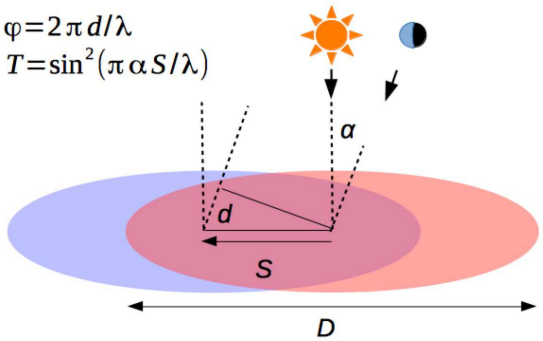

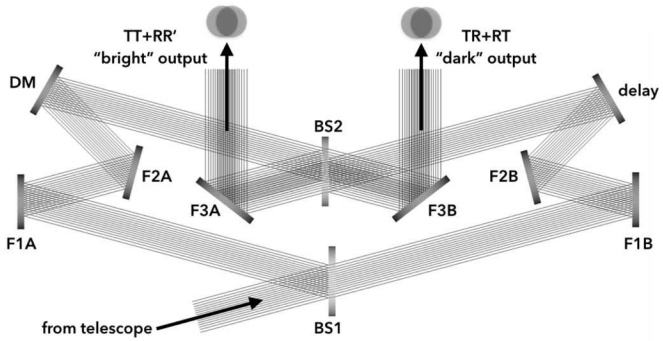

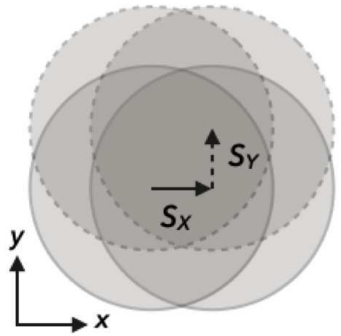

A VNC entry for the Segmented Coronagraph Design Analysis (SCDA) Study

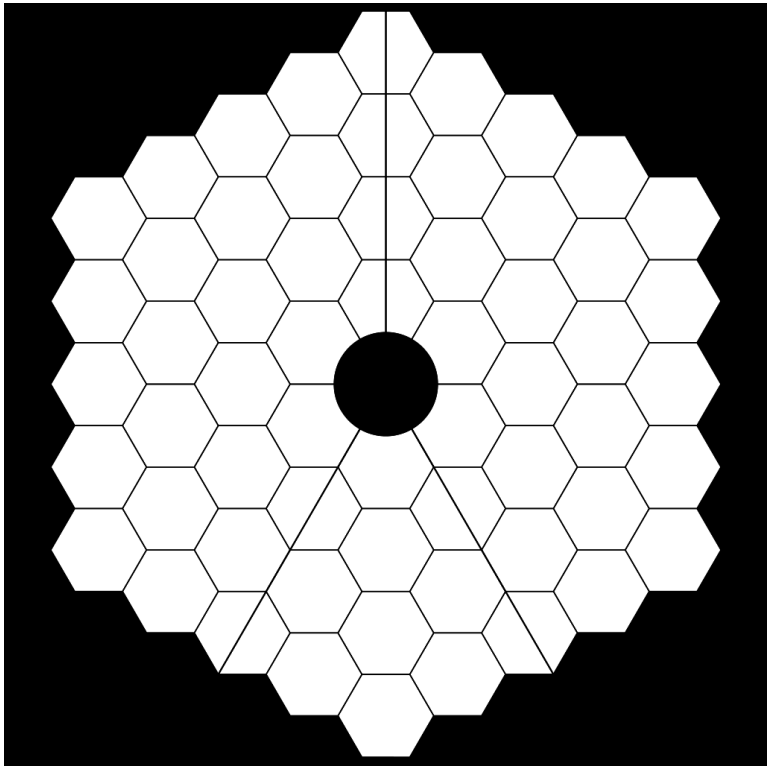

Assumptions:

- JWST-sized segments in 4-ring hexagonal array
- 11.7 m flat-to-flat aperture extent
- secondary obscuration ratio $\epsilon = 0.14$

VNC lateral shear nulling option 1: single segment shears at 60°

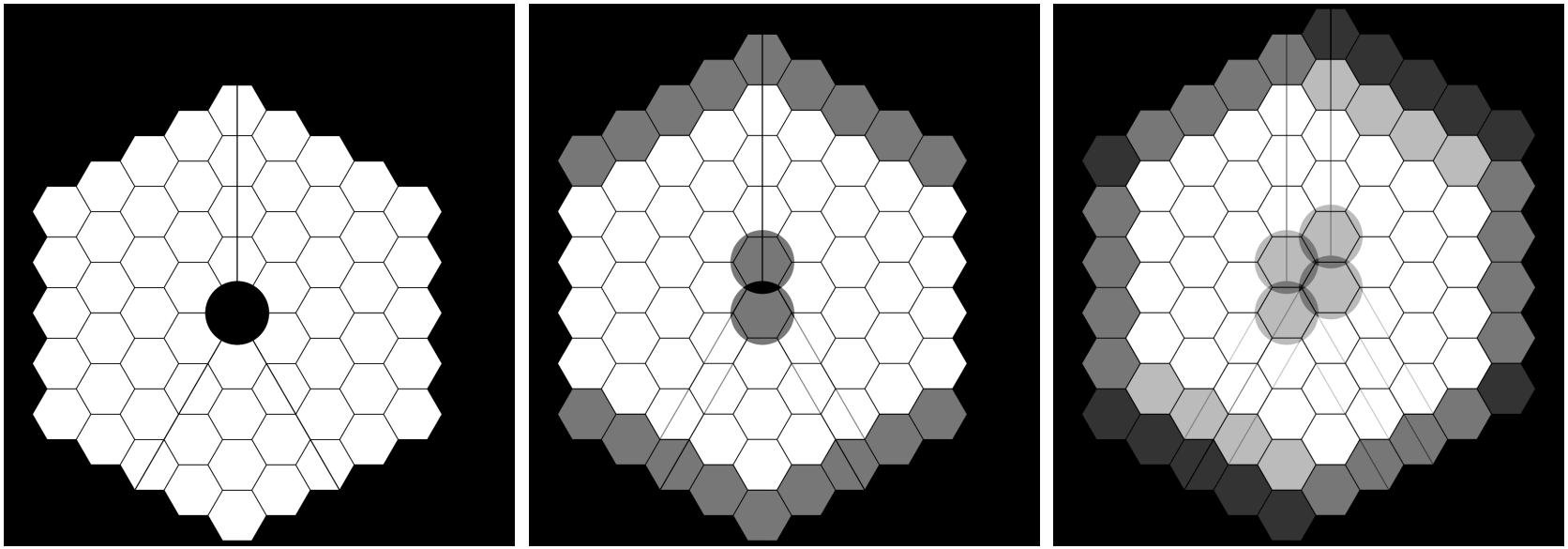

$$T(x,y) = \sin^2 \frac{\pi D y}{9\lambda} \sin^2 \frac{2\pi D(\sqrt{3}x+y)}{18\lambda}$$

$$\text{IWA} = 3.3\lambda/D$$

First transmission maxima at $(\pm\frac{9\lambda}{2\sqrt{3}D}, \pm\frac{9\lambda}{2D})$ and $(\pm\frac{27\lambda}{2\sqrt{3}D}, \mp\frac{9\lambda}{2D})$

VNC lateral shear nulling option 2: two parallel single segment shears

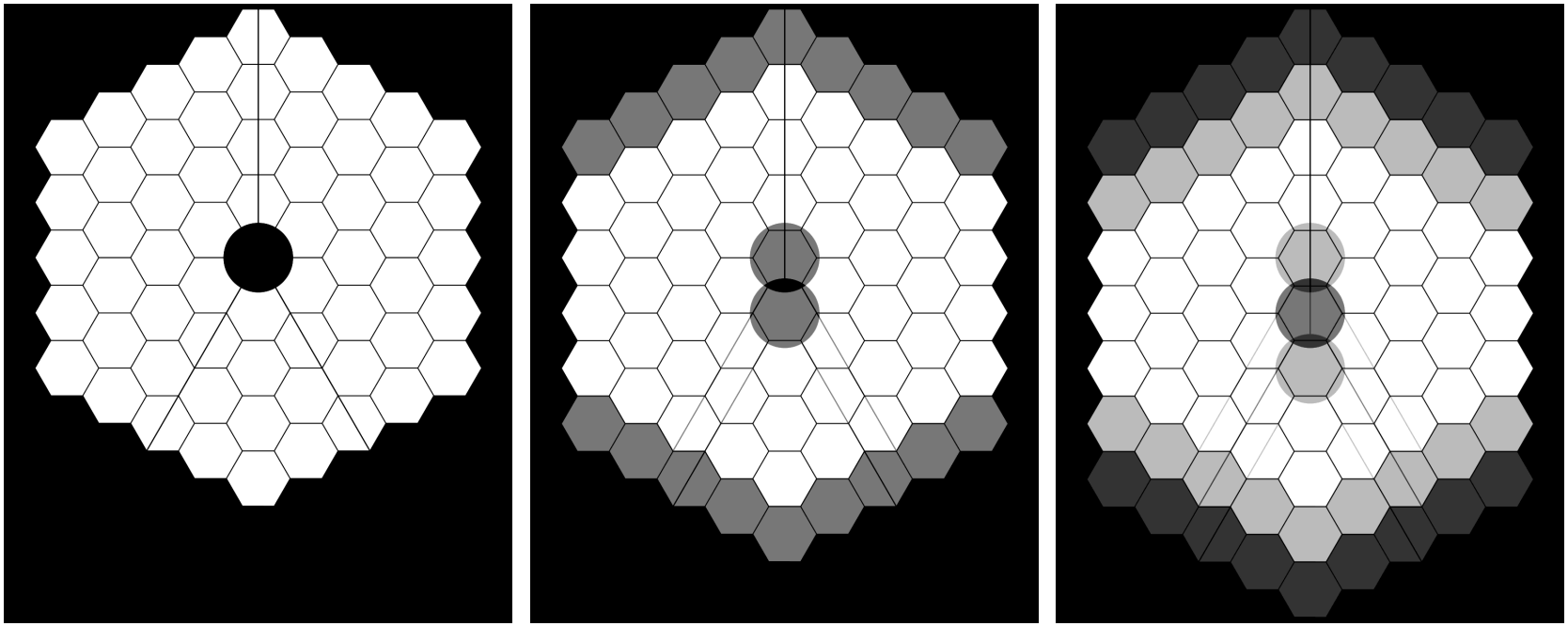

$$T(x,y) = \sin^4 \frac{\pi D y}{9\lambda}$$

$$\text{IWA} = 2.86\lambda/D$$

First transmission maximum at $4.50\lambda/D$

Fundamental performance following two shears

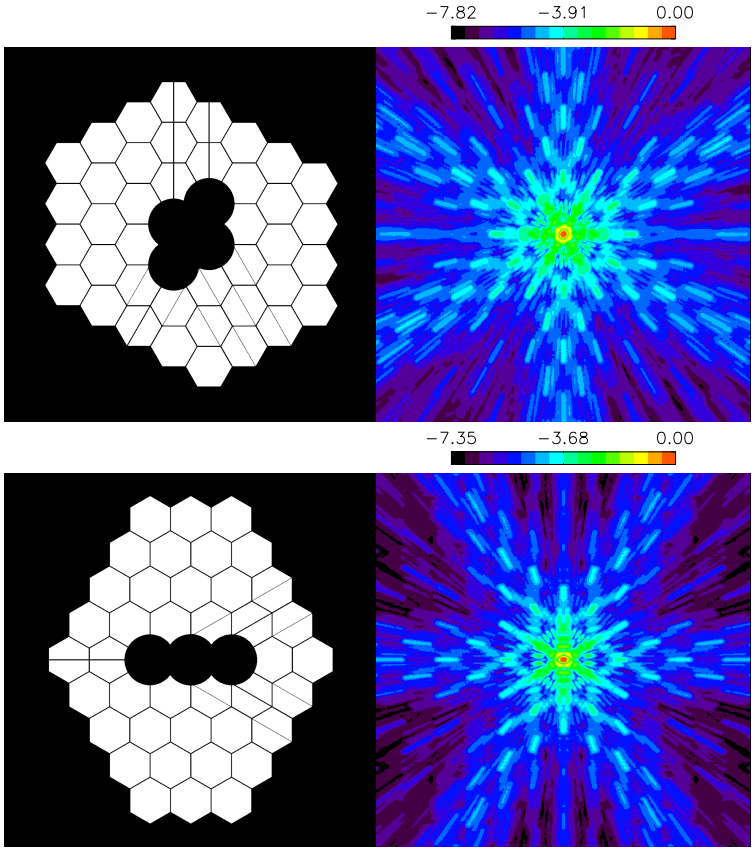

Left: Pupil image at Lyot stop; *Right:* normalized log-scale Aperture Spread Function (ASF)

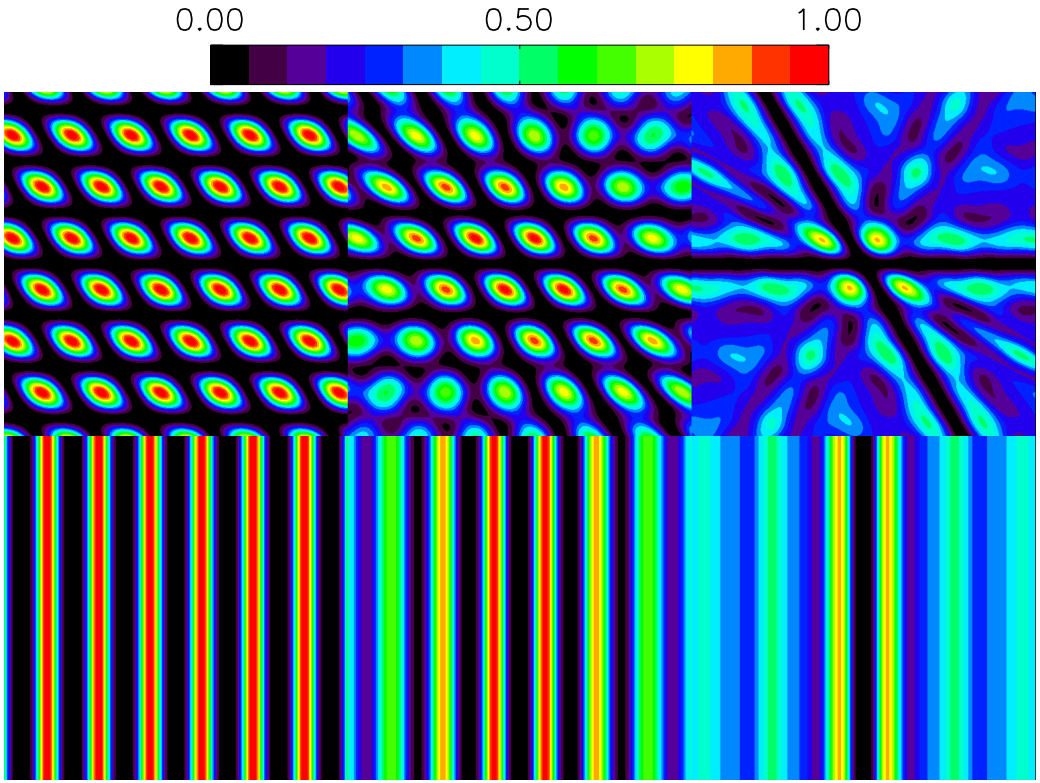

- Interferometric transmission only
- Single, dual parallel, and dual orthogonal $D/9$ shears
- no geometric aperture or bandpass multipliers
- monochromatic, 27%, and 66% bandwidths
- $\lambda_o = 750\ nm$, D=11.7 m, and OWA=$30\lambda/D$

Target Accessibility

Accessibility of habitable zones around A, F, G, K, and M stars within 30 pc of Earth based on system resolution, contrast, and photometric capability with the following assumptions:

- 11.7-m 4-ring hexagonal aperture
- Central $\lambda = 0.76$ µm (O_2)
- 10% spectral bandwidth
- 5% total throughput
- θ^4 stellar suppression
- D/9 linear shears
- 0.5 mas pointing
- $3\lambda/D$ inner working angle (IWA)
- $30\lambda/D$ outer working angle (OWA)
- PSF$\propto\rho^{-2.5}$

*Approximately $10-20$ of the systems plotted will transit.

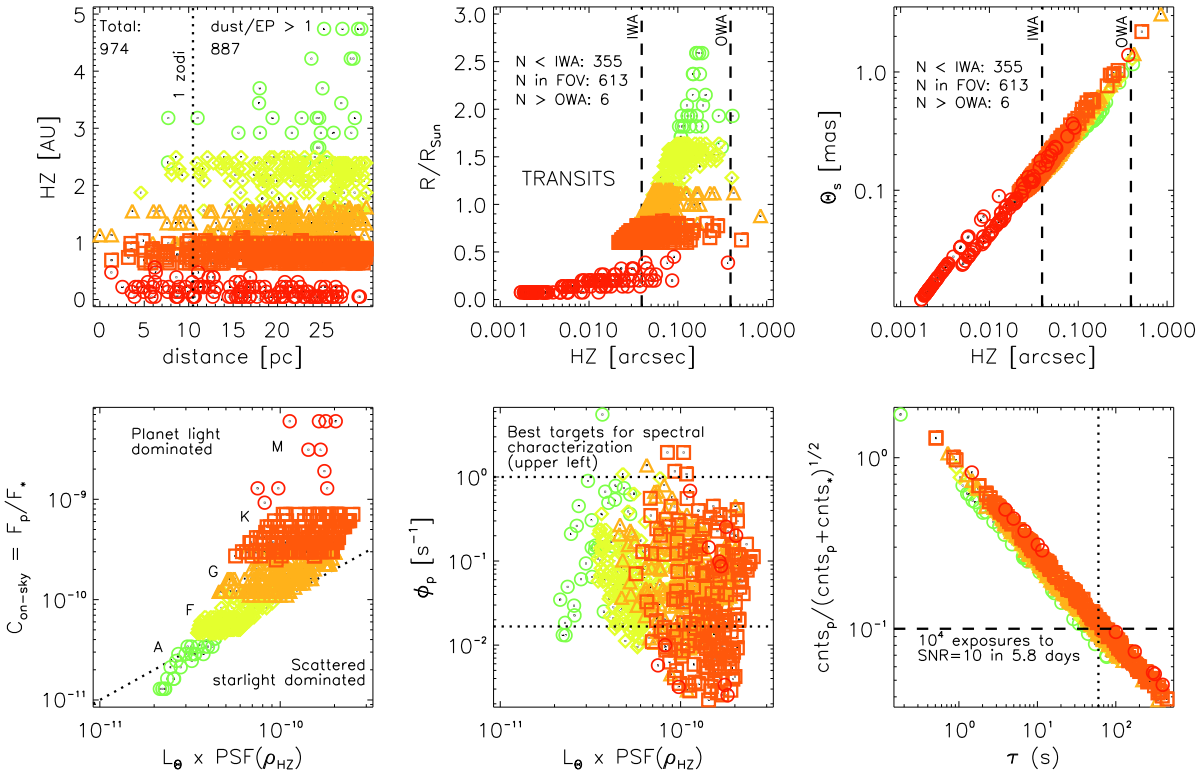

Random contrast and separation of Earth-like planets around stars within 30 pc

- Working with GSFC intern Andrew Eberhardt to model statistics of habitable zone detection
- Require follow-up to observe multiple epochs and place upper contrast brightness limits of non-detections

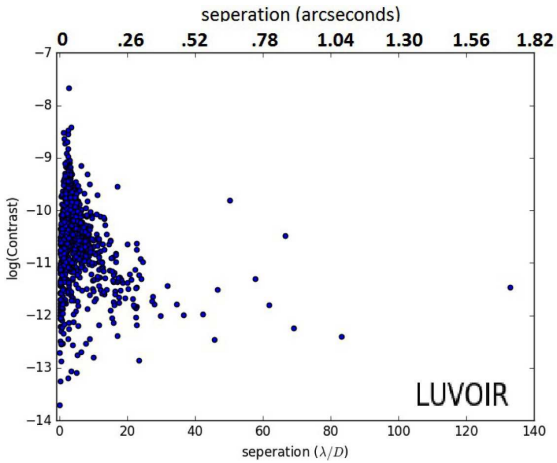

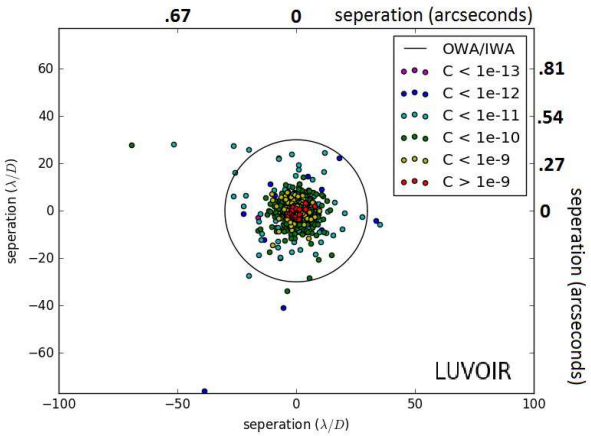

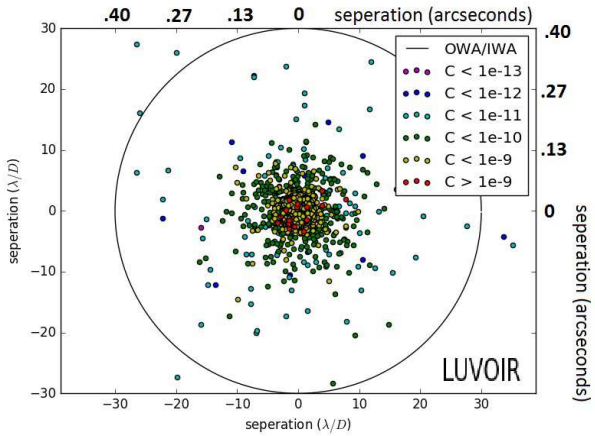

The Visible Nulling Coronagraph (VNC) & Segmented Aperture Interferometric Nulling Testbed (SAINT)

Funding: SAT/TDEM (PIs – M. Clampin, R. Lyon, M. Bolcar), IRAD, and SIF

5+ years team: Michael Helmbrecht (Iris AO), Pete Petrone (Sigma Space)

Recent contributions: James Corsetti (551/U Rochester), Bill Danchi (667), Dan Dworzanski (Optimax), Joe Howard (551), J. Scott Knight (BATC), Corina Koca (544), Marc Kuchner (667), Andy Lea (SGT), Tim Madison (551), Eric Mentzell (551), Ian Miller (LightMachinery), Kevin Miller (551), Teresa Sheets (587), Ron Shiri (551), Patrick Thompson (551), Gene Waluschka (551), Garrett West (551), Brandon Zimmerman (551)

Recent interns: Marlin Ballard (spring, summer 2016), Andrew Eberhardt (summer 2016, spring 2017), Joey Ulseth (spring 2016), +3 out of 5+ accepted so far (summer 2017)

Visible Nulling Coronagraph TDEM-10/TDEM-13 "laundry list" (slide 1 of 2)

Issue	Root Cause	System Effect	Mitigation Path
Mount instabilities and dark channel optics	Shifts and/or slow drift in e.g. DM mount, aft-optics frictionless zoom lenses, and 1/2" post-mounted components between measurements and after chamber loading following external alignment checks; an overly complicated imaging relay	Dark channel PSF shifting and Strehl degradation as well as chromatic aberration; reference beam tilt and path errors that can be observed on both bright and dark detectors, confounding coarse human-in-the-loop and automated fine control routines	Simplify aft-optics design, use more rugged mounts, and remove unneeded actuation – the aft-optics were redesigned in May 2016 and ruggedizing effort began in June 2016 excepting code and calibration needed for filter wheel, DONE
Deformable Mirror	Amplifier to device calibration is suspected to have drifted, manifested by observed irregular (not flat) fringe pattern when the DM is set to zeroes	A subset of individual segments reach the limit of control or exhibit significant non-linear response during automated phasing and fine control	Install a fully-functional DM and its calibrated amplifier that have been held in reserve DONE; the DM and amplifier that have been used will be reecalibrated for future use*
Delay stage	Backlash error in absolute stage positioning on the order of 1–2 **μ**m is observed using both human-in-the loop stepping and automated fringe tracking; creep is suspected	While the stroke of the PZT used for fine actuation is adequate to compensate for absolute errors, slow creep may be a source of drift away from the central null fringe during fine controls	~~Quantify settle time needed following coarse stepper actuation before attempting fine controls~~; explore incorporation of a hybrid slip-stick/PZT actuated coarse/fine delay mechanism PI Piezowalk installand and operating
Vacuum chamber	A limited number of access ports necessitates a six-way cross that 1) encumbers cabling and 2) introduces a torque on the system and its passive isolation	Optical mounts are subject to being inadvertently bumped or snagged during cabling – alignment checks must in some cases be repeated external to the chamber; the torque mode introduces an unwanted resonance	Add ports to the chamber (drawing below) for simplified cable harnessing and a more symmetric load on passive vibration isolators/dampers DONE

Visible Nulling Coronagraph TDEM-10/TDEM-13 "laundry list" (slide 2 of 2)

Issue	Root Cause	System Effect	Mitigation Path
Achromatic phase shifters	Uncoated BK7 APS were selected for this demonstration following no-bids for multi-layer coating designs that yielded more favorable performance with a more high-purity glass option (Lithosil)	The theoretical retardance is marginally acceptable for meeting the Milestone goals, constituting a significant contribution to the leakage error budget	Fabricate a new set of APS with multiple orders of magnitude improved theoretical performance consisting of rhombs with single layer coatings on the TIR surfaces within fabrication capability; the design may enable a simplified approach to mounting that improves stability FY17 IRAD in progress
Control OS	The Windows XP OS that has been in use exhibits bus issues and does not guarantee latency of computer operations	Communications with detectors and amplifiers periodically fail at initialization or are lost during operation and must be reset; control bandwidth is compromised	Migrate to a system with 16 processor cores running Linux well underway
Fiber bundle array	Anamorphic pitch mismatch between fiber bundle arrays and their segmented DM counterpart has proven to be a difficult problem to address optically, requiring complicated relay schemes; transmission properties have yet to be characterized adequately to justify the added complexity needed for their incorporation	Complex wavefront control is performed with the DM alone, leaving segment figure errors uncorrected and no means for fine amplitude control	Characterization of several FBAs has been proposed as work to be performed in parallel to upcoming VNC efforts; if a candidate component is identified, a vacuum-compatible optical relay will be designed for their incorporation with the system layout designed and concentrated measurements to commence June-August 2017

Modifications to nuller fore- and aft-optics

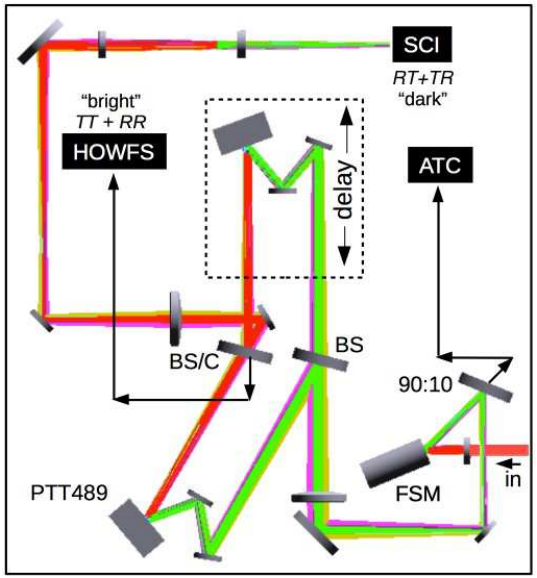

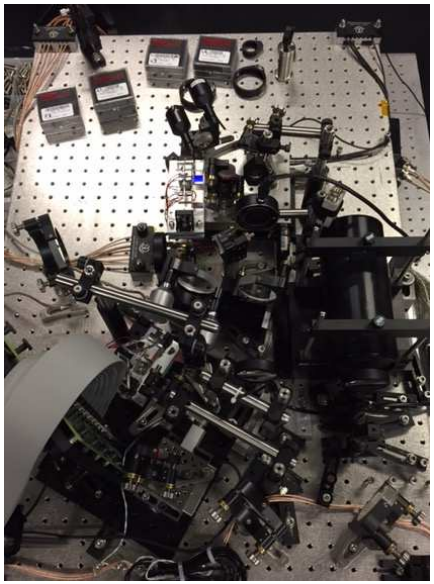

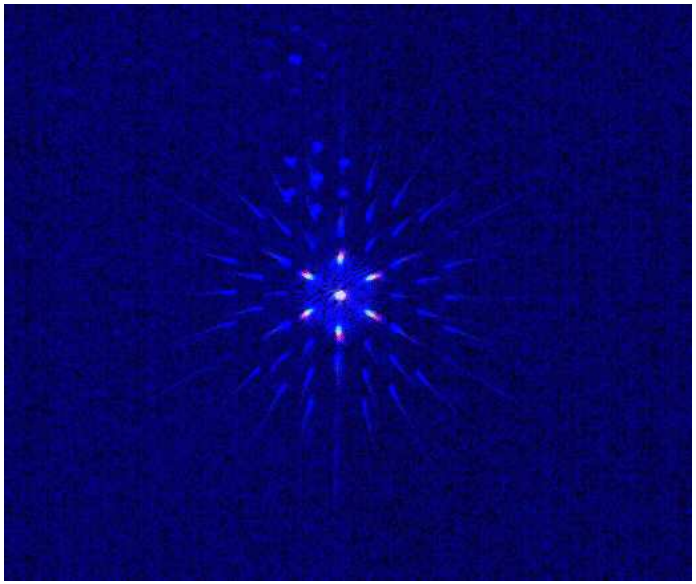

- Dark channel relay and imaging optics consisting of 5 zoom lenses, 1 diverger lens, and 7 fold mirrors have been replaced by three achromatic doublets and three fold mirrors and a Barlow lens. The last fold and Barlow are out of plane and not shown in the raytrace.
- Reduction of optics to improve stability, vacuum compatibility, and increase throughput
- A source module (right in above photo) will be replaced by the fine pointing system (FPS) consisting of a beamsampler (or dichroic beamsplitter), fast steering mirror (FSM), and magnifying optics to an angle tracker camera (ATC).
- A bandpass of 525–750 nm is shown imaged on a detector with 5.7 $\times$ 5.7 µm pixels. The demonstration platescale is $\approx$ 14 pixels per λ/D and will use a frame size of 512 $\times$ 512 pixels ($\approx$ 36.6λ/D square) with 6.5 µm pixels.

The rebuilt Visible Nulling Coronagraph breadboard

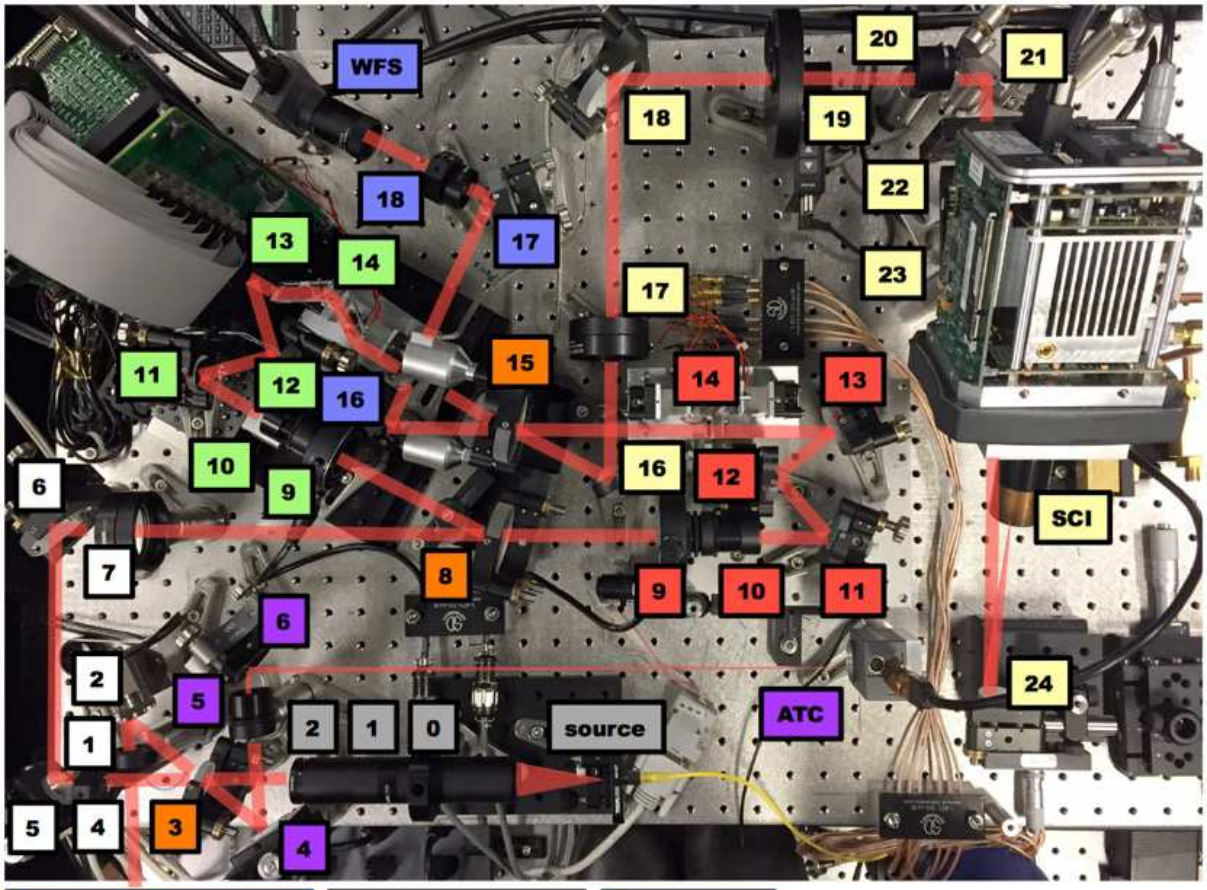

All-active Iris AO PTT489 DM control demonstrated on Linux machine

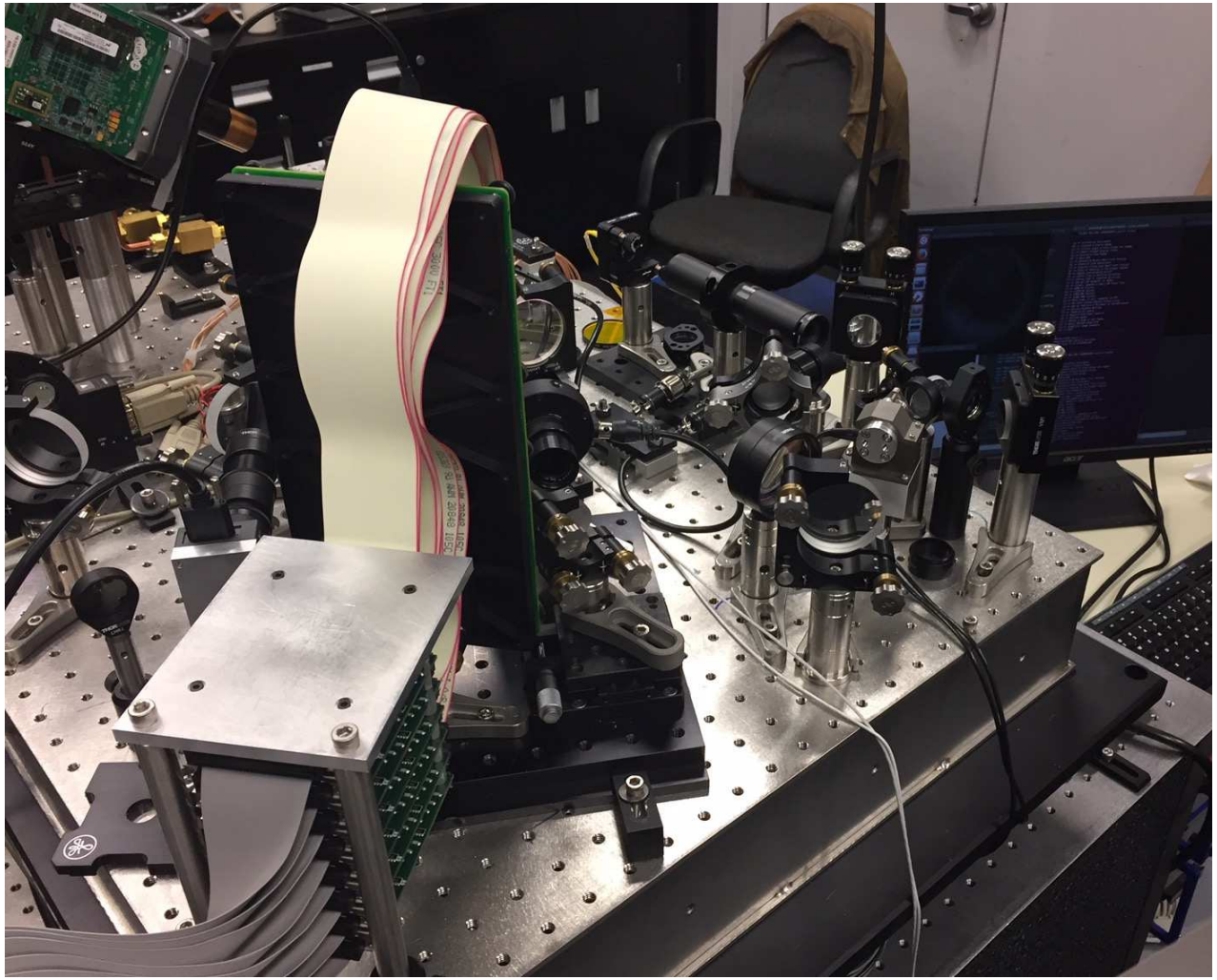

New delay line stage and "W" assembly

- Hybrid long travel (10 mm) and sub-nm resolution stepper motor and piezoelectric transducer "piezo" (PZT) replaced by Piezowalk inchworm to achieve same range, but with 100-1000x better absolute positioning via servo control
- Procurement, fabrication, alignment, and software rewrite demonstrating basic control completed December 2016

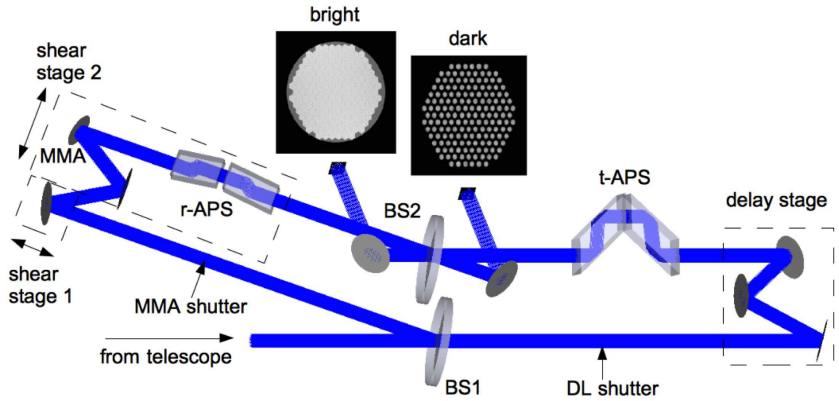

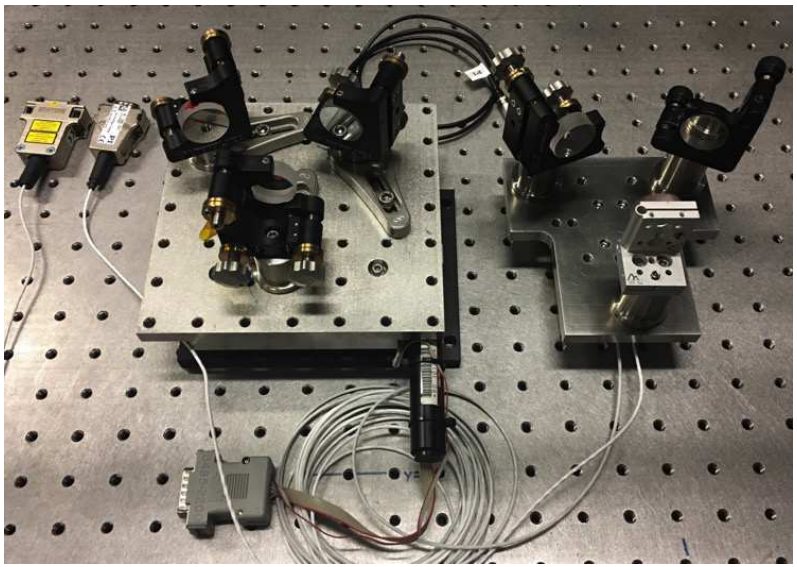

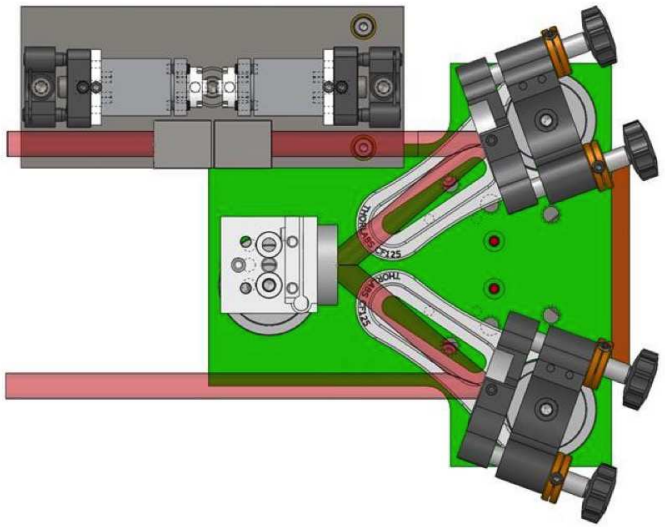

Vacuum chamber work complete

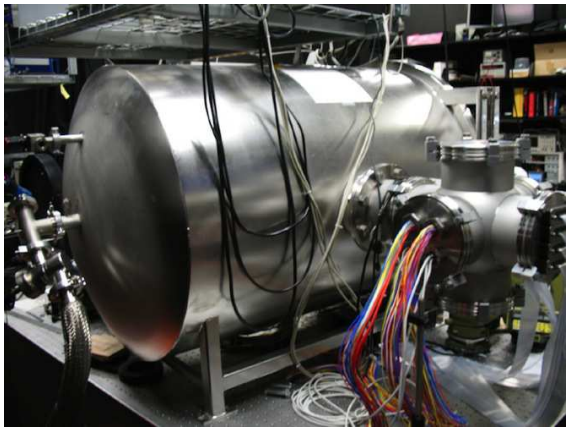

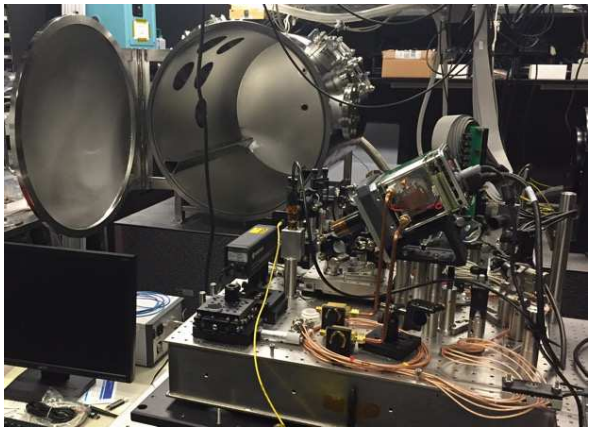

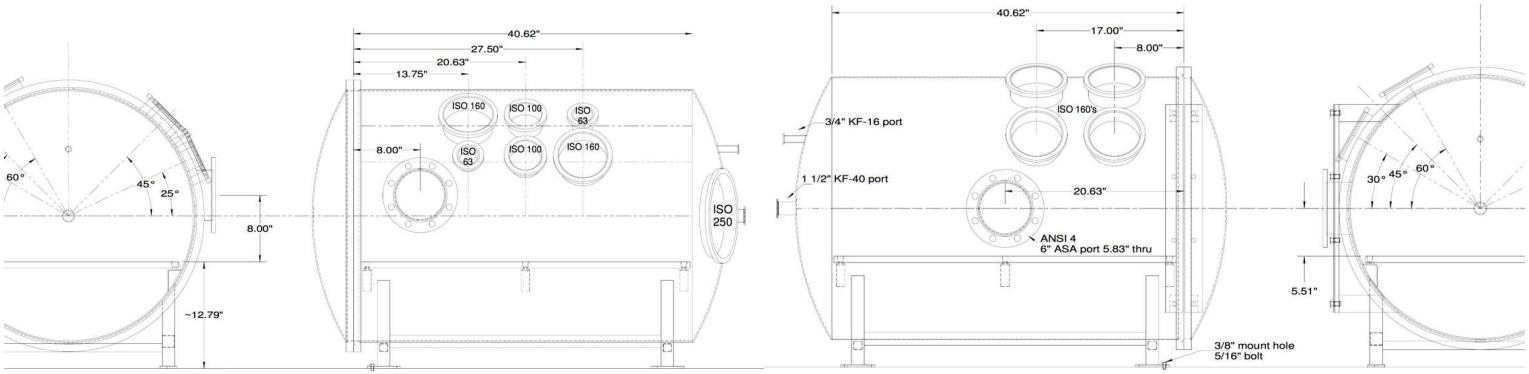

Pinholes and single mode fibers for higher contrast

- Enable complex (phase and amplitude) wavefront control by pairing a piston, tip, tilt deformable mirror with a single mode fiber array
- Single mode fibers filter residual phase errors that the deformable mirror cannot correct
- Amplitude control authority through tipping and tilting the deformable mirror segments to modify the overlap integral defined by beamlet and fiber geometry

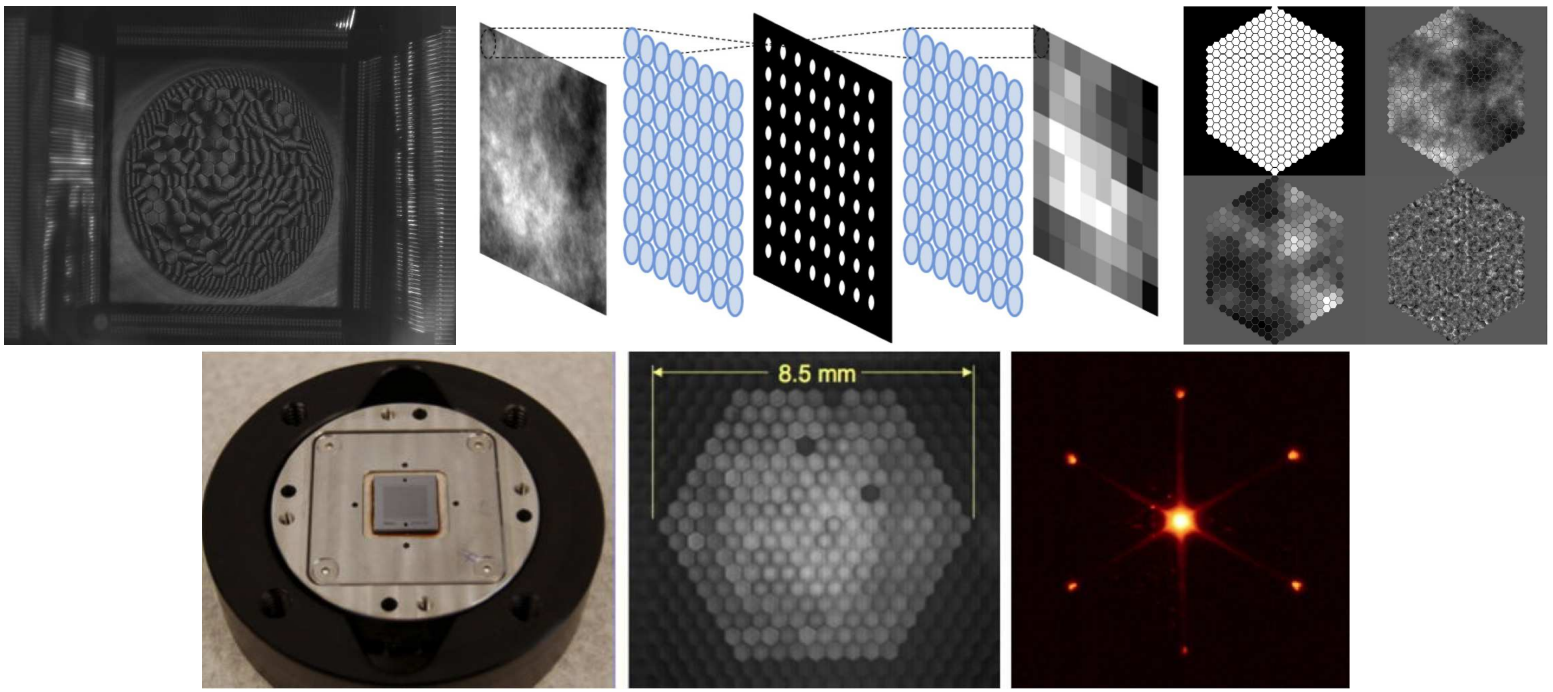

Single mode fiber array (SFA) testing

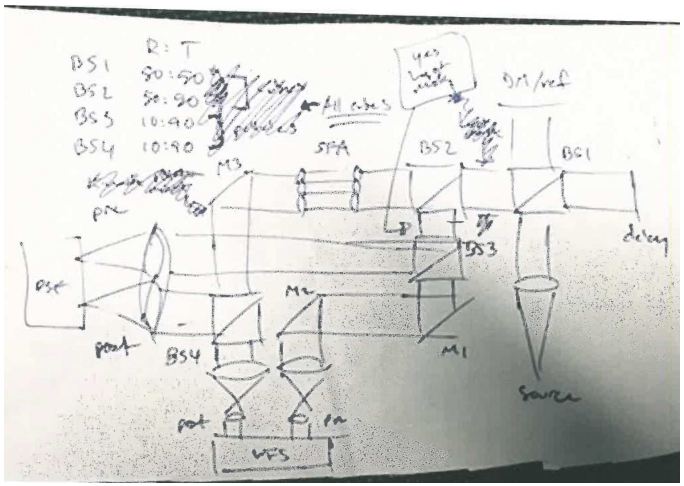

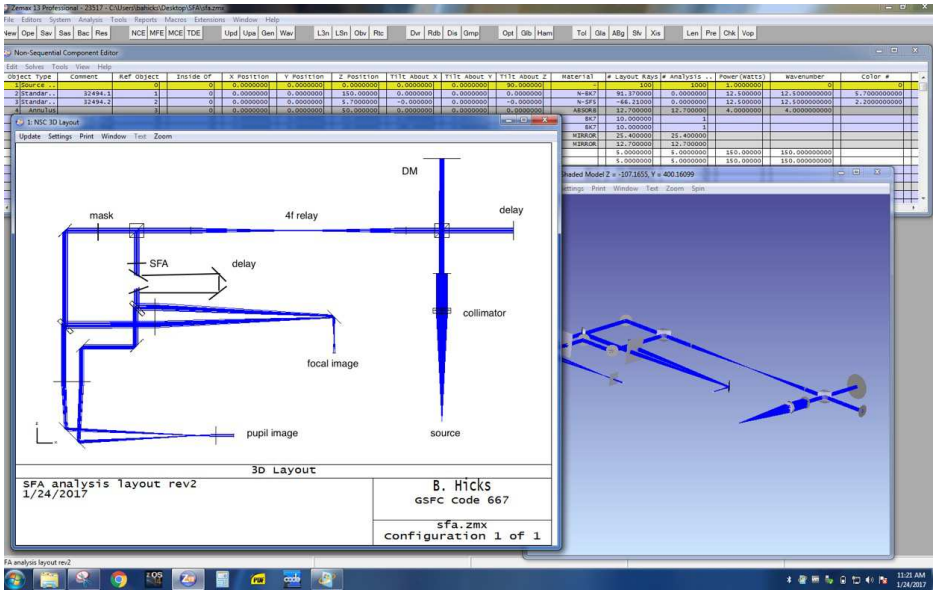

- A layout has been sketched, traced, and partially built
- A concentrated effort to characterize performance of SFAs will commence in May/June 2017

Radial shearing interferometer as a nuller

- Exploring the possibility of using a small imbalance in magnification between nuller "arms" to improve throughput and discovery space while achieving a reasonable inner working angle
- Schematic shows the concept using 2x magnification
- Hex apertures show 10% difference in magnification
- Challenges include matching field strength and path length while maintaining exit pupil plane coincidence

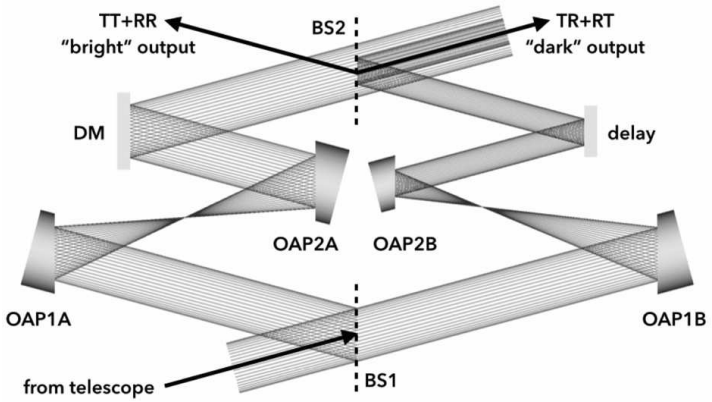

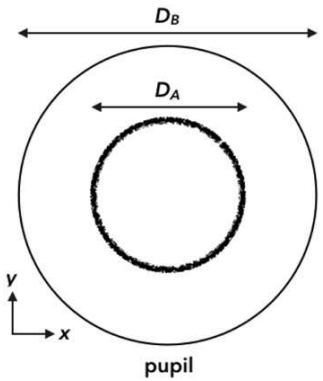

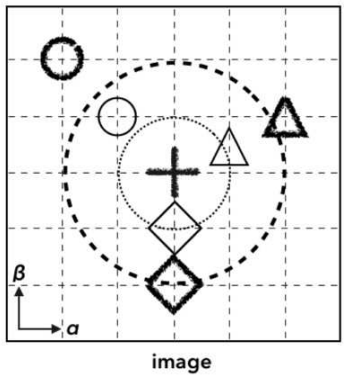

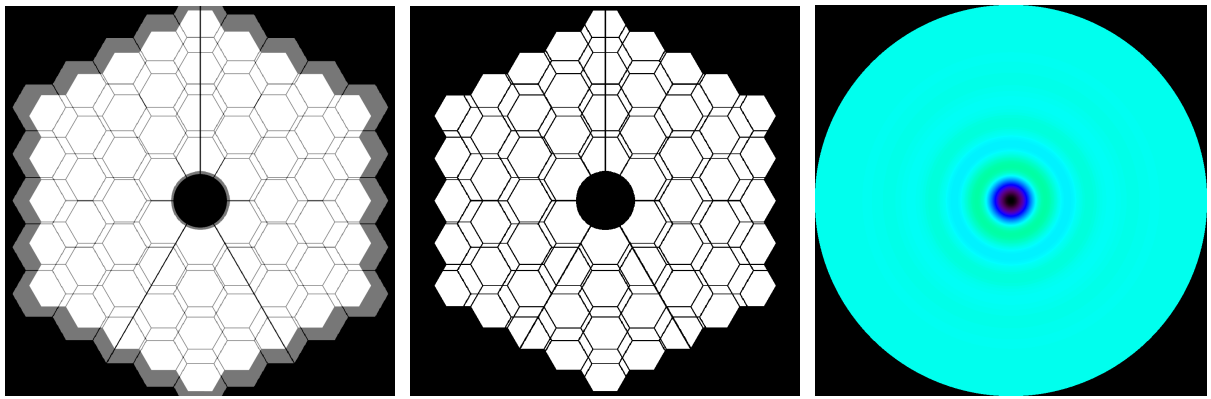

Segmented Aperture Interferometric Nulling Testbed (SAINT)

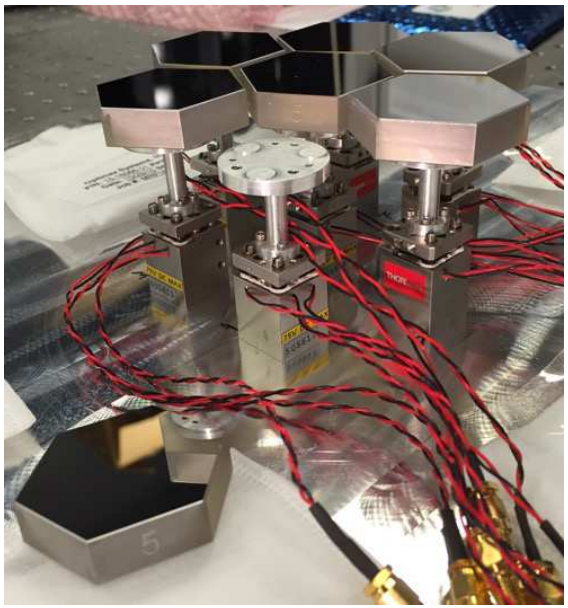

1) Active segmented mirror

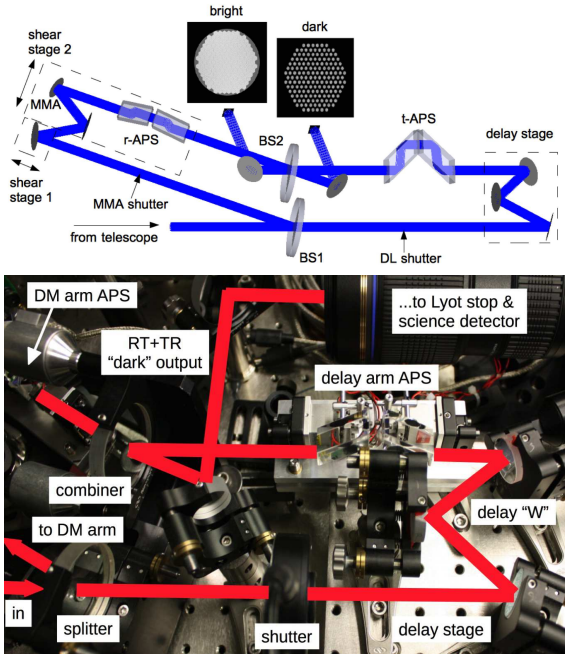

2) Visible Nulling Coronagraph

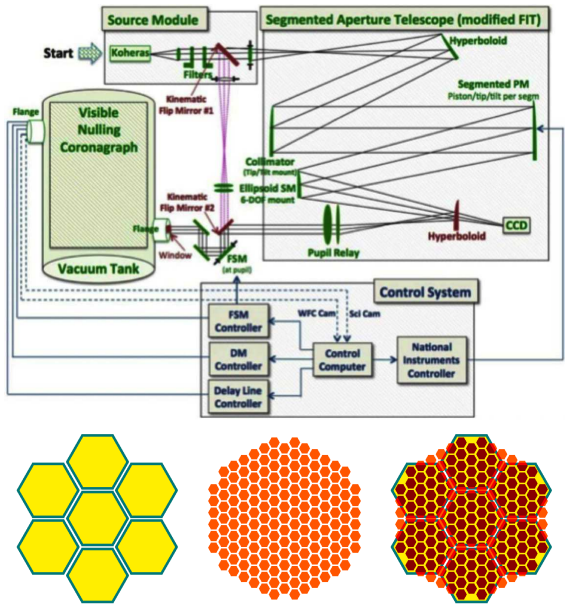

$1 + 2 = 3$) SAINT

Segmented Aperture Interferometric Nulling Testbed (SAINT)

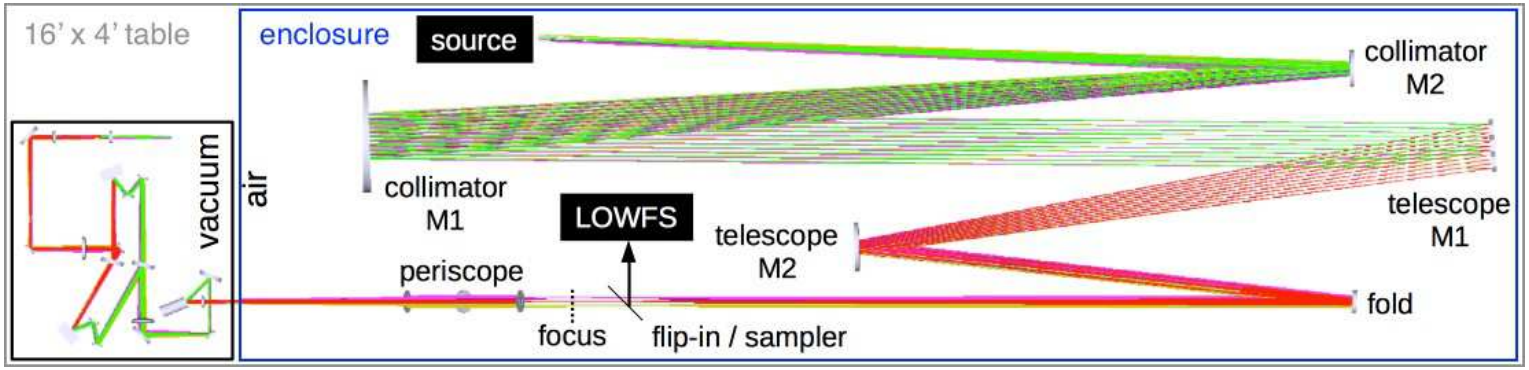

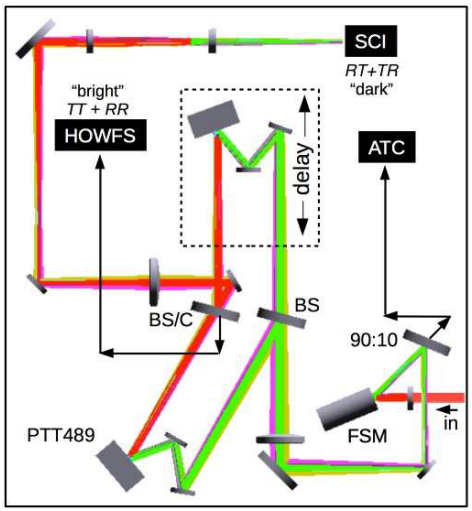

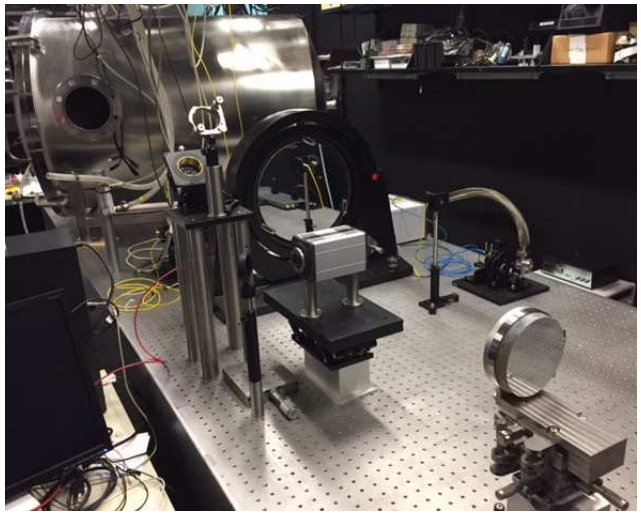

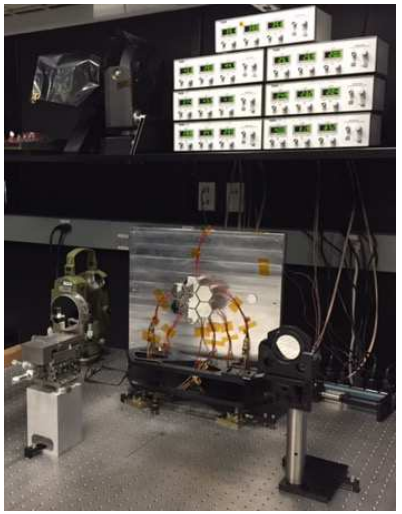

SAINT end-to-end dark channel Lyot mask & aperture spread function

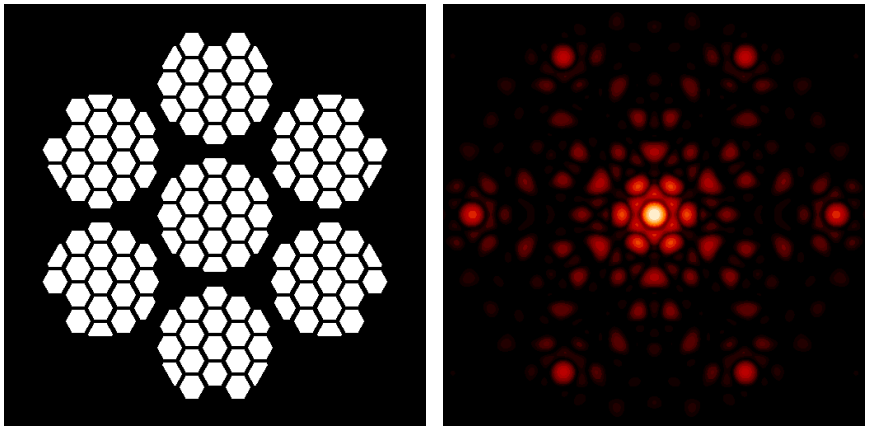

- Inner sidelobes at $3\lambda/D$ attributed to 1-ring segmented SAINT primary
- Outer sidelobes attributed to Iris AO, Inc. PTT489 7-ring hexagonal array deformable mirror
- A total of 127 out of 163 DM segments will be controlled

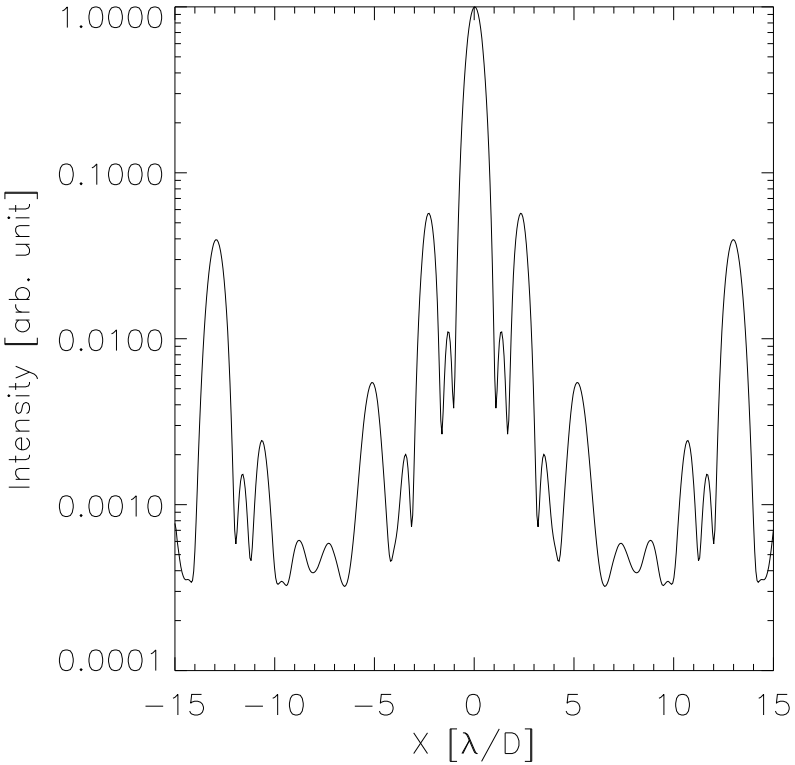

Intermediate piston/tip/tilt errors

Coarse adjustment using 100 TPI screws gives 1 μm piston, 15 arcsec tip/tilt resolution

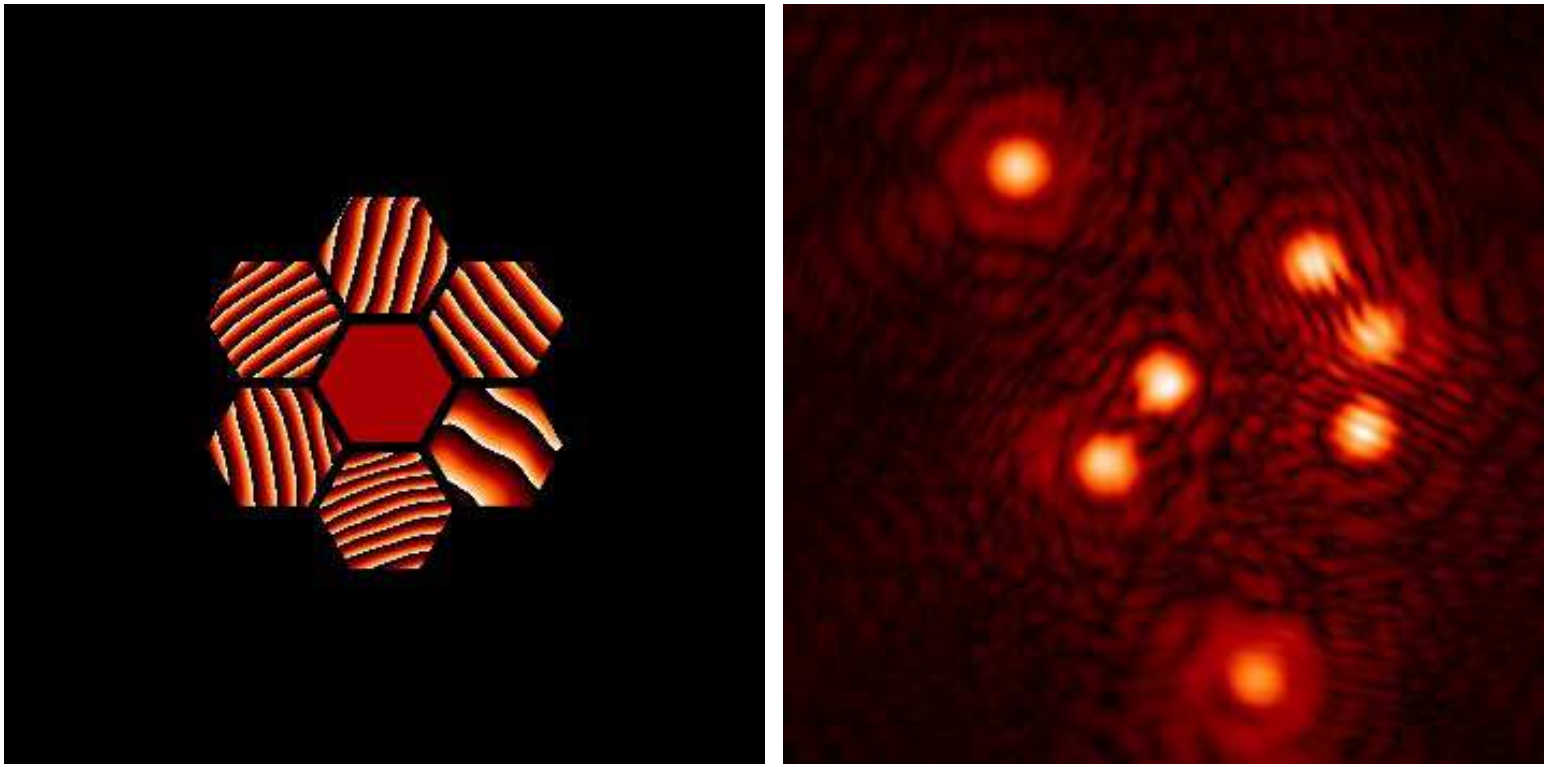

Hand-off to piezo fine controls with 7 μm piston and 120 arcsec tip/tilt range

Demonstrating fine array phasing

- Following coarse alignment using 100 TPI screws, switch to piezo controls
- Pairwise alignment of piston, tip, and tilt of the outer six segments relative to the central segment to minimize confusion
- Target aligned voltage matrix range of 37.5 ± 7.5 V (midrange $\pm$ control range/10)
- Segment pair subapertures (right) are 32 mm circles spaced at 42 mm
- Measured data uses 40 nm bandpass centered at 650 nm
- $\lambda/D = 4.2$ arcsec
- $\lambda/2B = 1.6$ arcsec

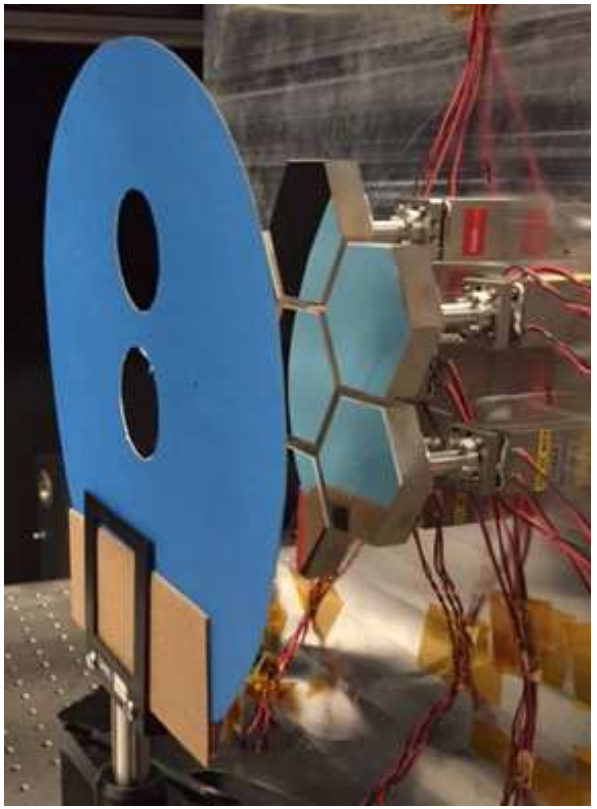

Segment tip sensitivity: two segments

Single segment surface tilts of 0, $\lambda/8$, $\lambda/4$, $\lambda/2$, and λ peak-to-valley

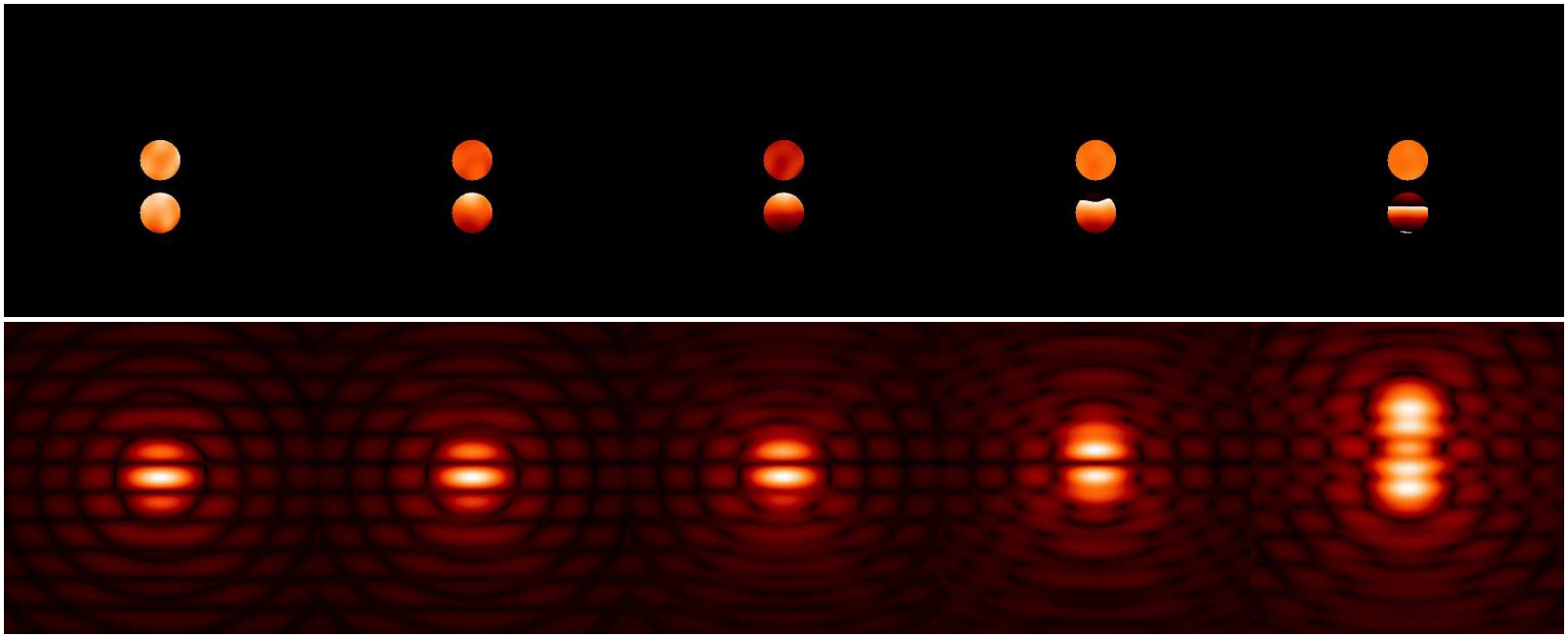

PSF intensity is stretched as $I^{1/4}$ and autoscaled in each frame

Segment tilt sensitivity: two segments

Single segment surface tilts of 0, $\lambda/8$, $\lambda/4$, $\lambda/2$, and λ peak-to-valley

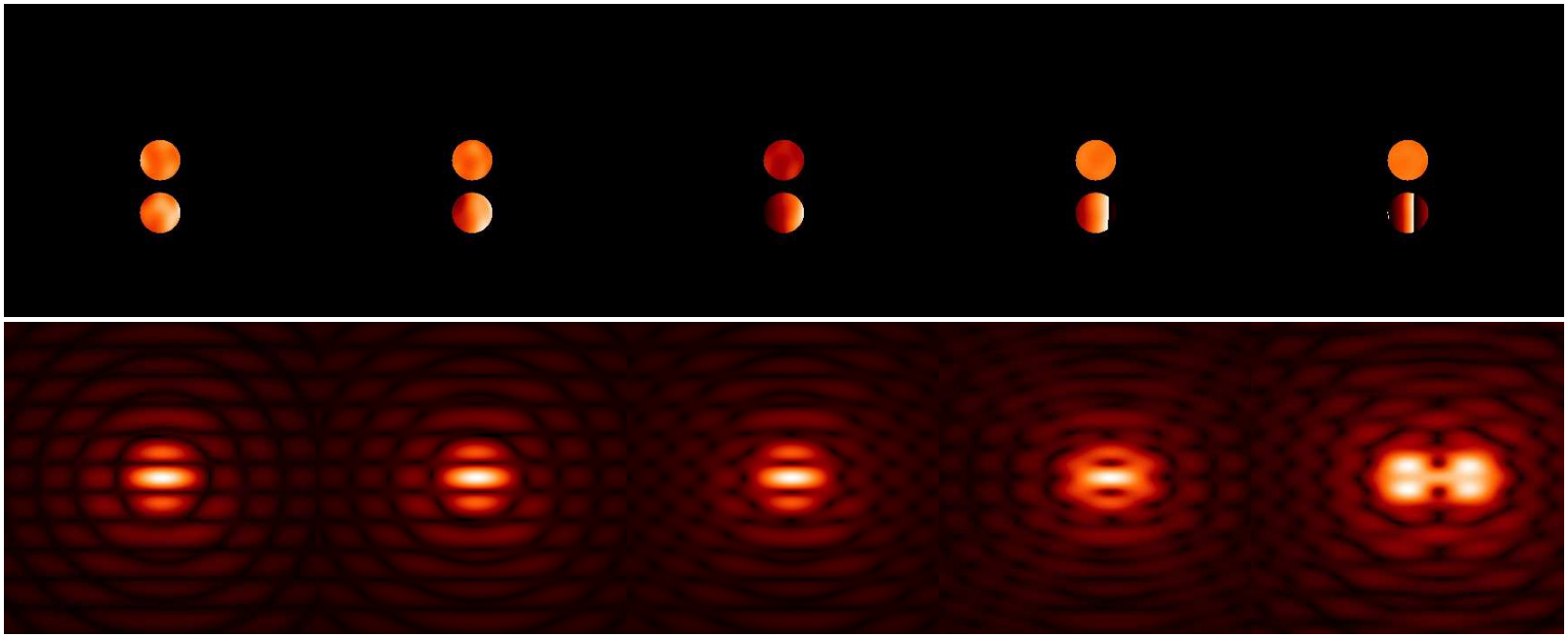

PSF intensity is stretched as $I^{1/4}$ and autoscaled in each frame

Segment tip sensitivity: full array

Single segment surface tilts of 0, $\lambda/8$, $\lambda/4$, $\lambda/2$, and λ peak-to-valley

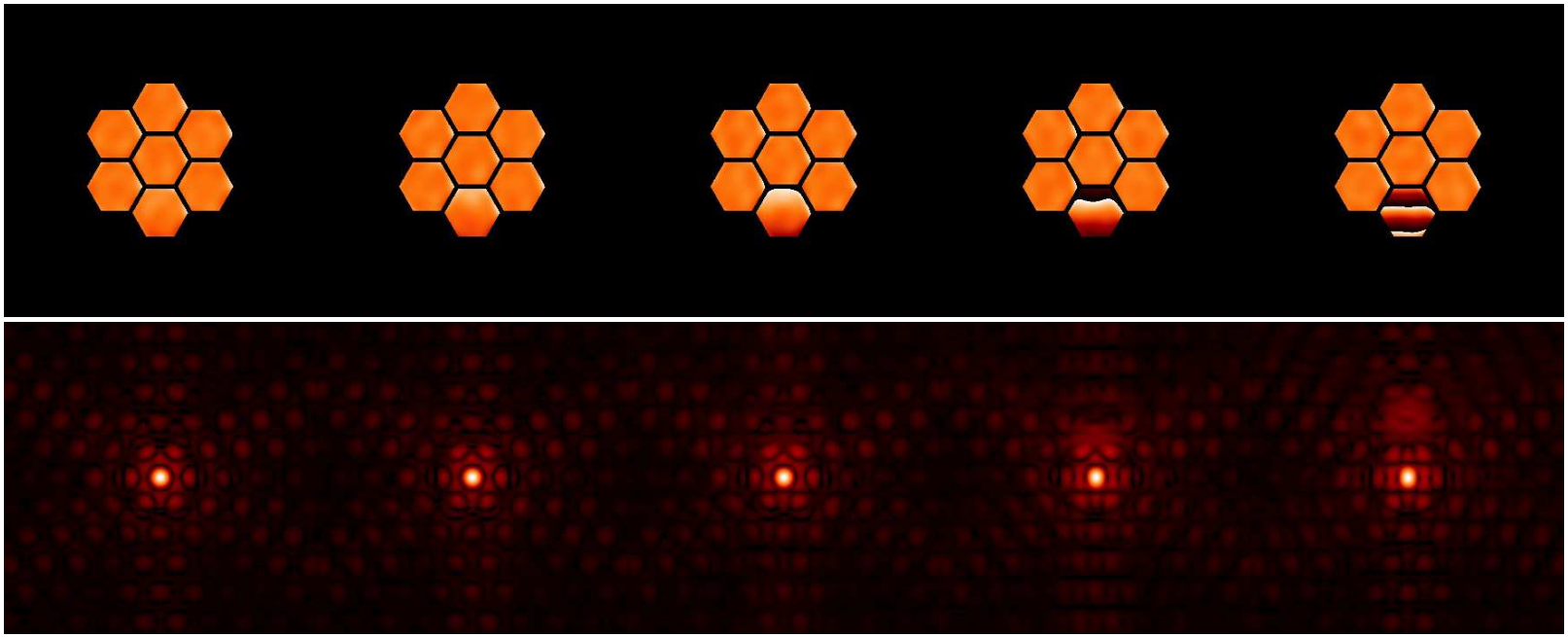

PSF intensity is stretched as $I^{1/4}$ and autoscaled in each frame

Segment tilt sensitivity: full array

Single segment surface tilts of 0, $\lambda/8$, $\lambda/4$, $\lambda/2$, and λ peak-to-valley

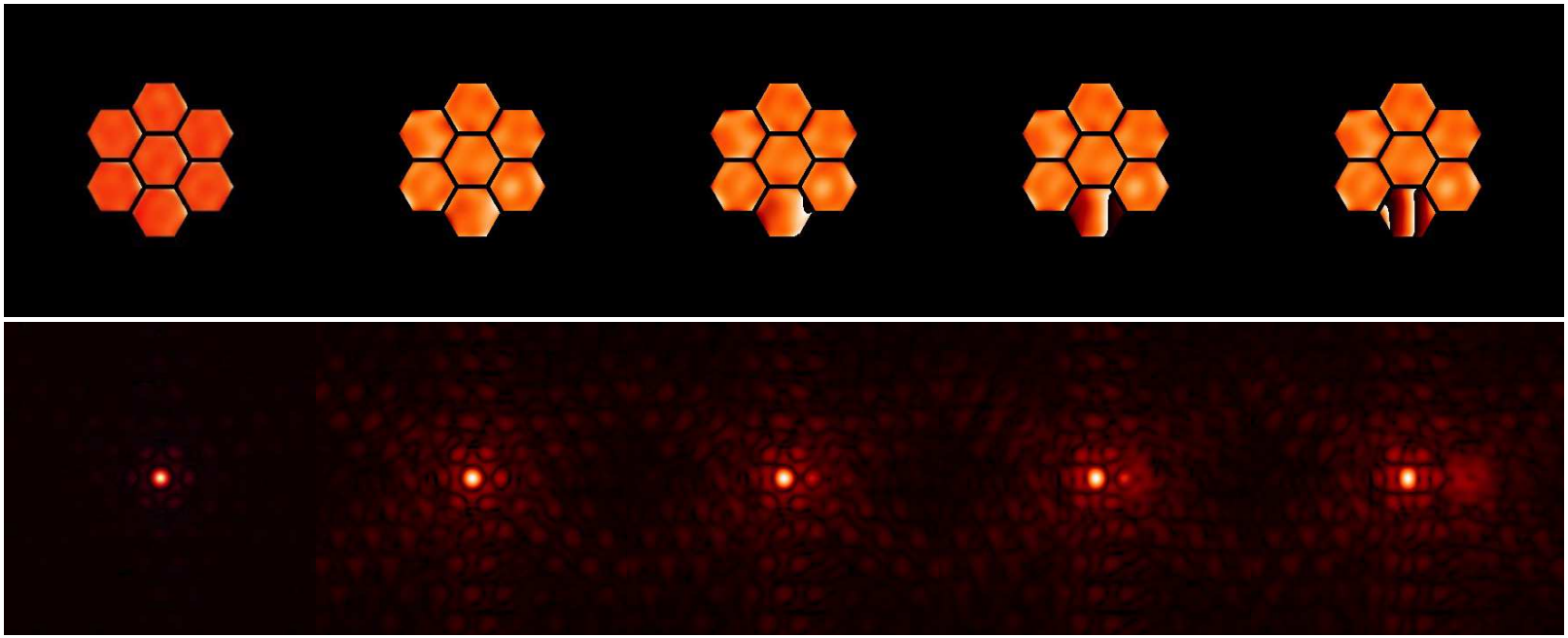

PSF intensity is stretched as $I^{1/4}$ and autoscaled in each frame

Simulation versus measurement: array actuator response calibration

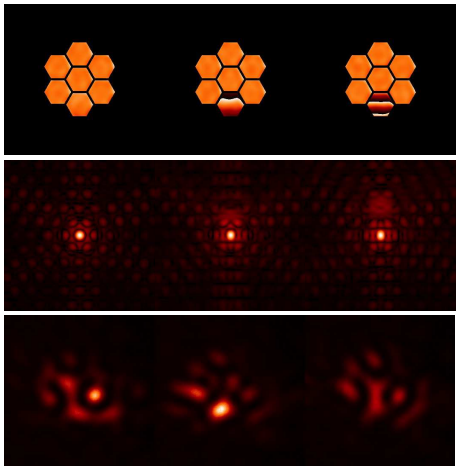

full tip (about x)

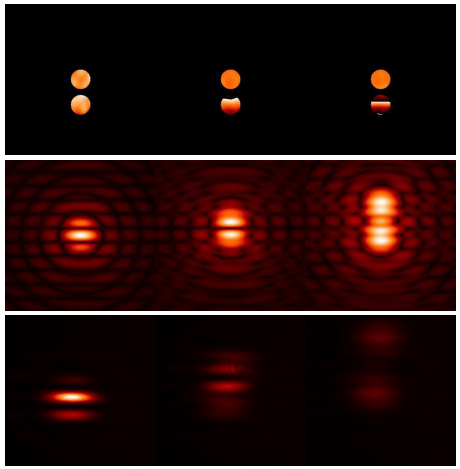

pair tip (about x)

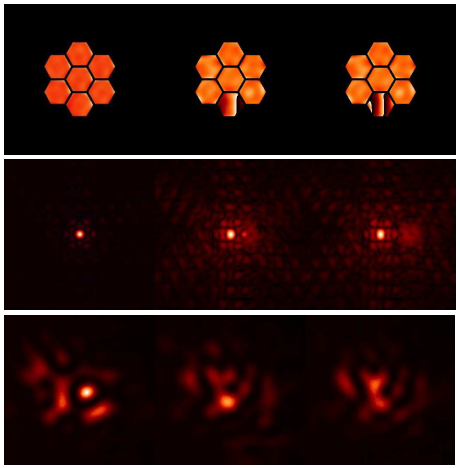

full tilt (about y)

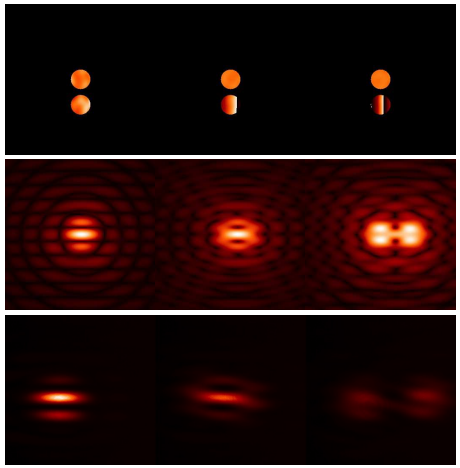

pair tilt (about y)

- Compare response of all 21 control degrees of freedom
- Discrepancies between simulated and measured PSFs due to static errors in array alignment (what this step will fix) and lab turbulence
- Simulations represent 0, $\lambda/2$, and λ PV tip/tilt surface errors (0, λ, 2λ tip/tilt wavefront error)
- Measured data corresponds to 0.0, 1.5, and 3.0 V amplifier control, which give 0, 2.4 and 4.8 arcsec rotations according to device specifications
- Segment pair subapertures (right) are 32 mm circles spaced at 42 mm
- Measured data uses 40 nm bandpass centered at 650 nm
- $1\lambda/D = 4.2$ arcsec

Vertex-sampled Shack-Hartmann approach to segment alignment sensing

- Sample vertices to maximize area being sampled
- Off-point one of the two outer segments initially to minimize confusion, then optimize coherent broadband intensity, then repeat for second outer segment
- Use segment straddling subaperture sampling scheme to track and correct slow drift in segment to segment alignment
- Counteract sources of drift, e.g., piezo amplifier control voltage drift

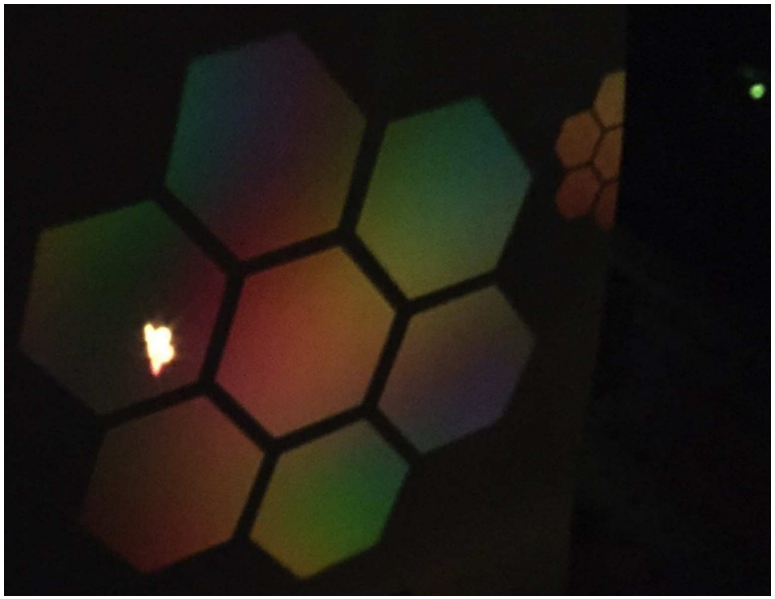

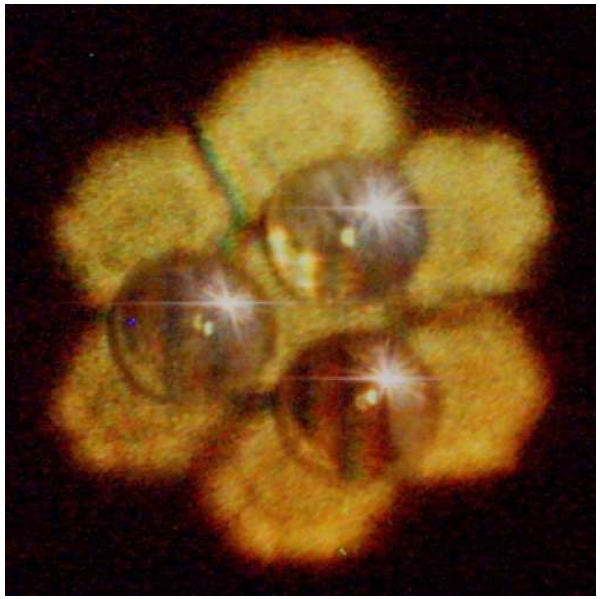

High frequency centroid jitter

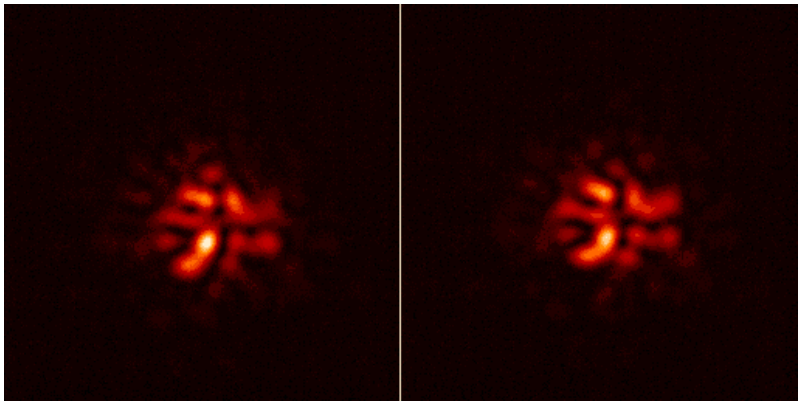

- Sampling at 800 fps
- $\approx$ 4 pixels per λ/D where $D \approx 120$ mm for the full array
- Center of mass centroid calculation
- As of yet unidentified peak near 28 Hz in addition to expected 60 Hz
- Next step is to add an enclosure to reduce jitter attributed to lab turbulence
- Enclosure panel material selected for its acoustic damping properties

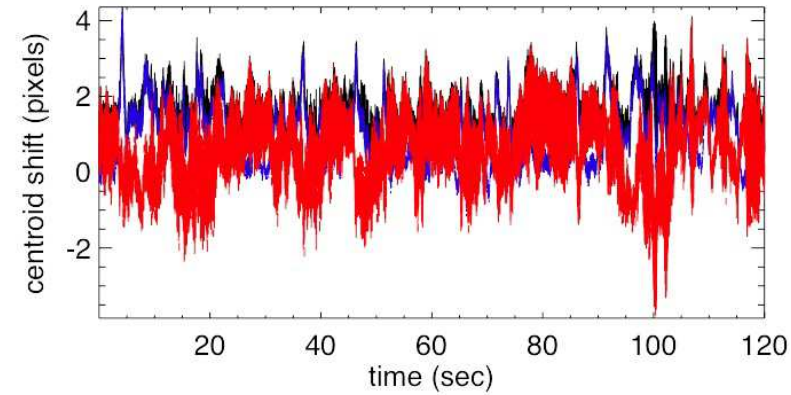

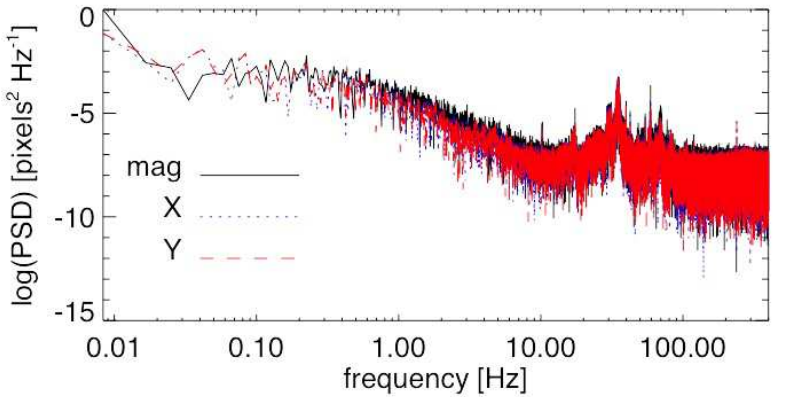

High-frequency PSF variability

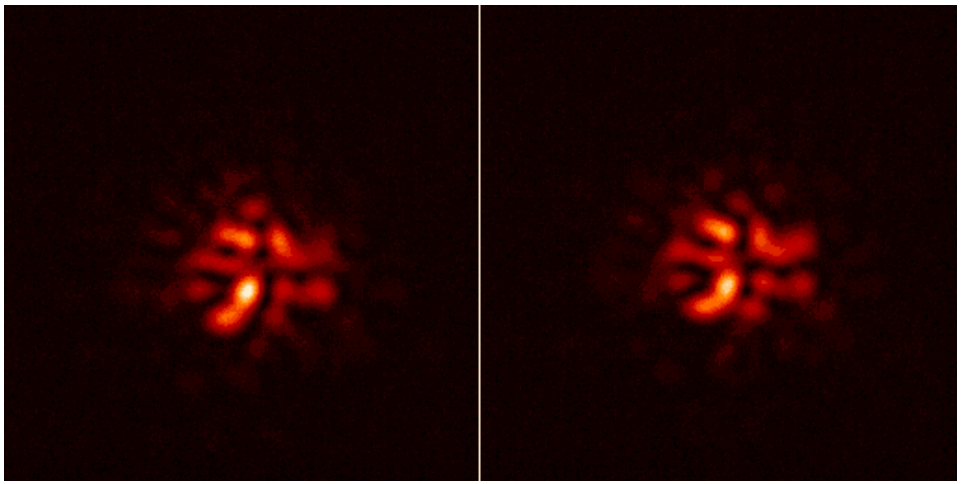

- Data on right comprises 94000 frames recorded at 800 fps
- The same data should be recorded once the enclosure is built around the air-side optics
- Additional efforts are required to quantify mechanical, acoustical, and turbulent jitter

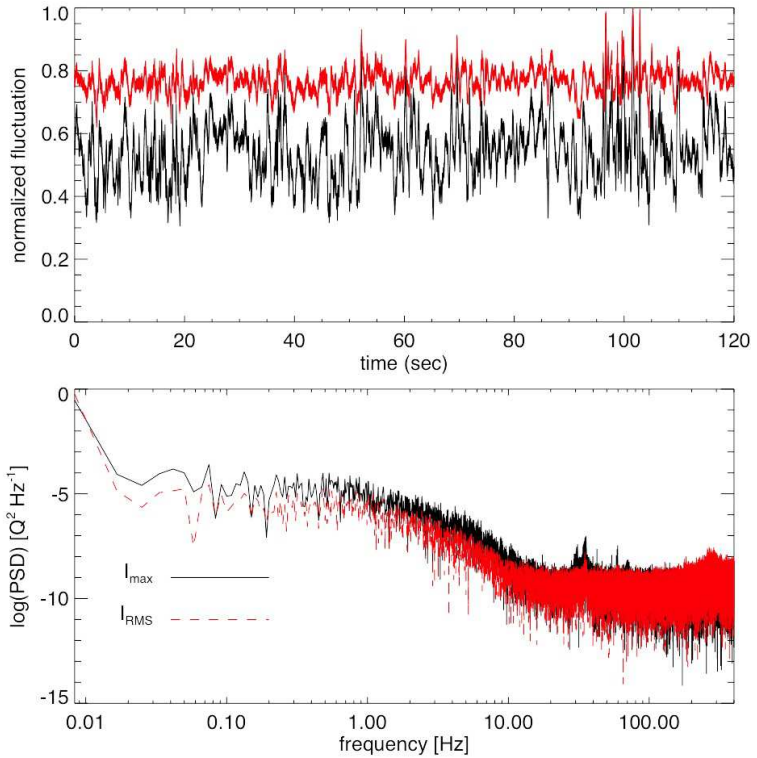

Long-period PSF evolution

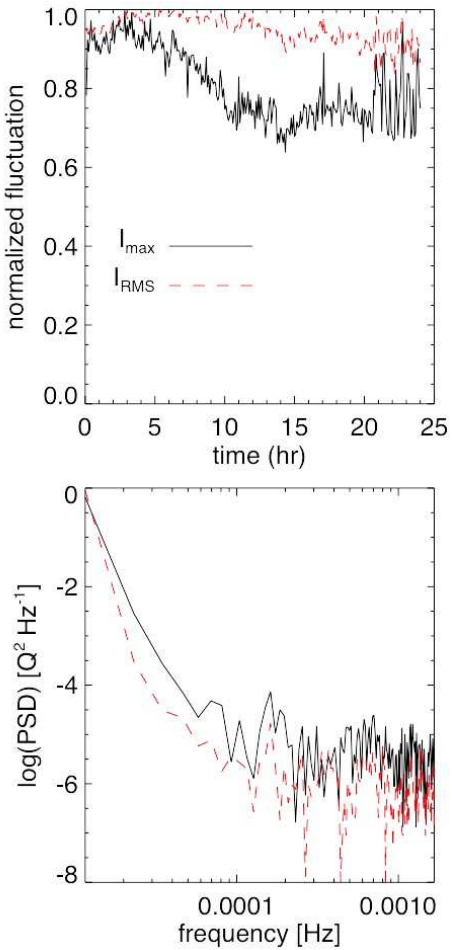

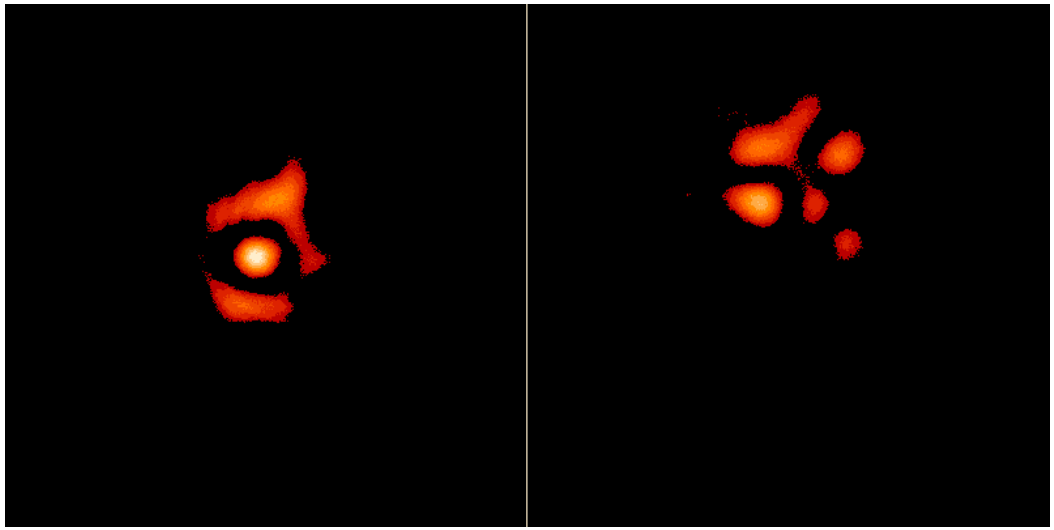

- Characterize slow drift in segment to segment alignment, evidenced by speckle intensity in first and final frames (above) spanning an hour time period
- Used to identify and mitigate sources of drift, e.g., piezo amplifier control voltages that can be monitored independently
- Select one or more metrics for monitoring and optimization, e.g., encircled energy or Strehl ratio
- Plots (left) show normalized time evolution and PSD of peak pixel intensity and the standard deviation of all pixel intensities

Next step: Fine Pointing System

The SAINT fine pointing system will couple the air-side segmented mirror array to the VNC

- To be developed in parallel to ongoing repeat demonstration of past VNC performance
- Initial work carried out by intern GSFC M. Ballard (U. Maryland)
- Incremental summer 2016 demonstration used an Arduino and pulse width modulation circuit for both driving both perturbing piezo piston/tip/tilt stage as well as the fast steering mirror (FSM)
- Demonstration grade FSM and its amplifier have been calibrated and are being integrated

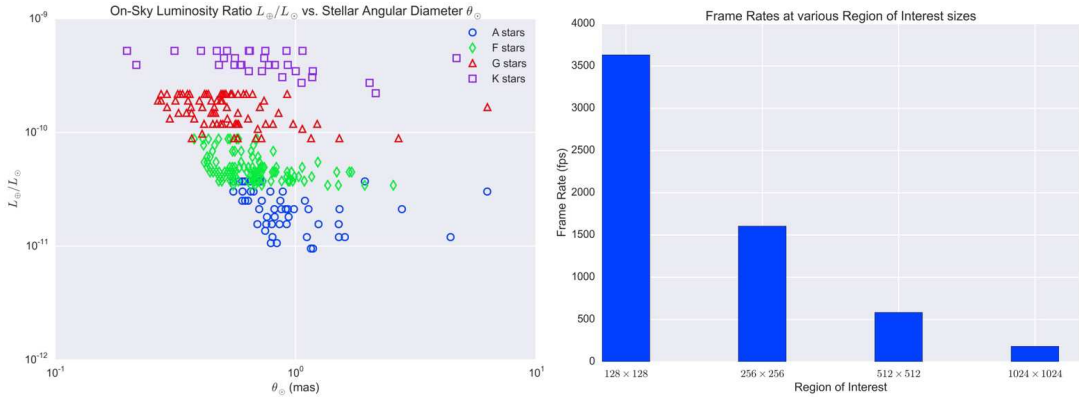

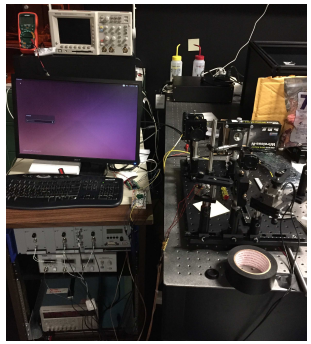

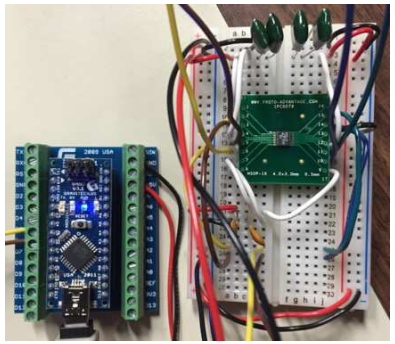

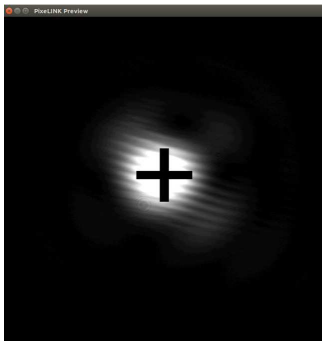

Thank you

- Nullers and masks are being developed at Goddard to achieve requisite contrast and resolution requirements for exoplanet direct imaging with complex aperture space telescopes
- Next top-level steps in SAINT/VNC development and demonstration:
  1. Demonstrate narrowband 10^{-8} contrast at $2\lambda/D$ with the rebuilt VNC (TDEM-13 Milestone #1.5)
  2. Demonstrate broadband ($\Delta\lambda = 40$ nm centered near $\lambda_o = 633$ nm) 10^{-9} contrast at $2\lambda/D$ with the rebuilt VNC (TDEM-13 Milestone #2.5)
  3. Demonstrate end-to-end(x4) alignment of SAINT, evidenced by simultaneous frame capture in both the 1) bright (HOWFS) and 2) dark (science) outputs of the VNC, a (stabilized?) spot on 3) the angle tracking camera (ATC), as well as Shack-Hartmann and/or a coherent full array PSF on 4) the LOWFS
  4. Demonstrate broadband ($\Delta\lambda = 20$ nm centered near $\lambda_o = 633$ nm) end-to-end 10^{-8} contrast at $4\lambda/D$ with the rebuilt VNC (TDEM-13 Milestone #3)